IEEE Access
Multidisciplinary | Rapid Review | Open Access Journal

Received March 2, 2020, accepted March 22, 2020, date of publication March 26, 2020, date of current version April 13, 2020.

Digital Object Identifier 10.1109/ACCESS.2020.2983451

Rationalized Sine Cosine Optimization With Efficient Searching Patterns

HUI HUANG[1,2], XI'AN FENG[1], ALI ASGHAR HEIDARI[3,4], YUETING XU[2], MINGJING WANG[5], GUOXI LIANG[6], HUILING CHEN[2], (Member IEEE), AND XUEDING CAI[7]

[1]School of Marine Science and Technology, Northwestern Polytechnical University, Xi'an 710072, China
[2]College of Computer Science and Artificial Intelligence, Wenzhou University, Wenzhou 325035, China
[3]School of Surveying and Geospatial Engineering, College of Engineering, University of Tehran, Tehran 1417466191, Iran
[4]Department of Computer Science, School of Computing, National University of Singapore, Singapore 117417
[5]Institute of Research and Development, Duy Tan University, Da Nang 550000, Vietnam
[6]Department of Information Technology, Wenzhou Polytechnic, Wenzhou 325035, China
[7]Division of Pulmonary Medicine, The First Affiliated Hospital of Wenzhou Medical University, Wenzhou 325000, China

Corresponding authors: Guoxi Liang (guoxiliang2017@gmail.com), Huiling Chen (chenhuiling.jlu@gmail.com), and Xueding Cai (xueding514@126.com)

This work was supported in part by the Natural Science Foundation of China under Grant 61702376, in part by the Zhejiang Provincial Natural Science Foundation of China under Grant LSZ19F020001, in part by the Science and Technology Plan Project of Wenzhou, China, under Grant 2018ZG012 and Grant G20190020, in part by the Graduate Scientific Research Foundation of Wenzhou University under Grant 3162018024, in part by the Zhejiang University Students Science and Technology Innovation Activity Plan under Grant 2019R429043, in part by the key scientific research project of Wenzhou Polytechnic under Grant WZY2019004, and in part by the service and technology innovation project of Wenzhou science and technology association under Grant 2019KXCX-RH07.

ABSTRACT Even with the advantages of the sine cosine algorithm (SCA) in solving multimodal problems, there are some shortcomings for this method. We observe that the random patterns utilized in SCA cause an increasing attraction toward local optima. This study developed a rationalized version of this technique to deal with several representative benchmark cases with different dimensions. The improved algorithm combines the chaotic local search mechanism and Lévy flight operator with the core trends of SCA. The new variant is named as CLSCA. The Lévy flight with long jumps is adopted to boost the exploratory tendencies of the algorithm, while the chaotic local search mechanism is used as a local search for the destination point, which helps to further enhance the exploitation capability of SCA. Therefore, a suitable equilibrium between the exploration and exploitation can be kept in the CLSCA by two embedded patterns. To investigate the effectiveness and strength of the developed method, the CLSCA was tested on many benchmark functions, including different types of tasks such as single modal, multi-modal, hybrid, and composition functions. We compare the CLSCA with well-known optimizers, like particle swarm optimization (PSO) algorithm, grey wolf optimizer (GWO), SCA with differential evolution (SCADE), opposition-based SCA (OBSCA), fuzzy self-tuning PSO (FST_PSO), chaotic salp swarm algorithm (CSSA), and Chaotic whale optimizer (CWOA). Numerical experimental results demonstrate that the exploratory and exploitative properties of the classical SCA are clearly improved. The experimental results also show that our improved CLSCA is a better technique for different kinds of optimization tasks.

INDEX TERMS Sine cosine algorithm, optimization, chaotic local search, Lévy flight.

I. INTRODUCTION

With the expansion of tools and soft computing methods, the community is facing many real-life tasks that need to feasible solutions using mathematical models [1]–[7]. However, metaheuristic methods (MAs) and machine learning models are effective substitute techniques for tackling practical problems [8]–[11]. Inspired by nature or physical problems, numerous intelligent algorithms have been widely used to solve optimization problems [12]–[16]. These intelligent algorithms often show better results than traditional gradient-based algorithms [17]. Some of these

The associate editor coordinating the review of this manuscript and approving it for publication was Hao Luo.

intelligent algorithms, like the whale optimization algorithm (WOA) [14], [18]–[21], bat algorithm (BA) [22], [23], differential evolution (DE) [24], fruit fly optimization algorithm (FOA) [25]–[29], moth-flame optimization algorithm (MFO) [30]–[33], ant colony optimization algorithm (ACO) [34], [35], grey wolf optimizer (GWO) [36]–[38], grasshopper optimization algorithm (GOA) [39], fireworks algorithm (FWA) [40], particle swarm optimization (PSO) [41]–[43], salp swarm algorithm (SSA) [44], Harris hawks optimization (HHO) [45]–[47], and bacterial foraging optimization (BFO) [15], [48]–[50], have tackled various optimization cases. In 2016, Mirjalili [51] proposed a new metaheuristic algorithm, namely the sine cosine algorithm (SCA). In the SCA, mathematical sine and cosine functions are used to conduct the exploration and exploitation of the search space. Simplicity and efficiency have been demonstrated in terms of convergence and computational efforts. As a result, the SCA has attracted extensive attention from the research community in various fields [52]–[55].

In the SCA algorithm, sine and cosine functions are employed to update a set of candidate solutions [51], which balances the trade-off between exploration and exploitation in the search space. However, like other meta-heuristic algorithms, SCA is easy to fall into a local minimum that it appears in the computational effort required to find the global optimal solution. This happens for the reason that operators applied in the process of exploration do not work well to analyze the search space. Therefore, in the related literature, many improved SCA variants have been researched [52]–[56]. In 2017, Abd Elaziz *et al*. [57] proposed a developed SCA using opposition-based learning (OBL) as a mechanism to generate more accurate solutions. The proposed algorithm has been tested using benchmark functions and constrained engineering design optimization problems, and the results supported the efficacy of the proposed approach for finding the optimal solutions in complex search spaces. Sindhu *et al*. [58] put forward an improved SCA (ISCA) schema to select the best features for boosting the classification accuracy, and their results indicated that the ISCA could achieve a better classification performance with a fewer number of features. A new multi-objective SCA (MO-SCA) based on the search technique of the SCA was developed by Tawhid and Savsani [59], and their simulation results confirmed that the developed MO-SCA was effective and more suitable in dealing with multi-objective benchmark problems and multi-objective engineering design problems. For fast and efficient tracking, a hybrid SCA with the Cauchy and Gaussian mechanisms was developed by Kumar *et al*. [60] for a single sensor-based maximum power point tracking (MPPT) algorithm. The performance of the developed method has been compared with that of the conventional dual (voltage and current) sensor-based MPPT strategy and several recent state-of-the-art techniques, and the results of such comparisons validated the performance of the proposed technique. Issa *et al*. [61] introduced a hybrid algorithm called ASCA-PSO, which was based on the combination of SCA and PSO. Experimental results have demonstrated the performance of the proposed method for settling several benchmark problems and the real-world problem of a pairwise local alignment algorithm. In 2018, Chegini *et al*. [62] proposed a novel hybrid algorithm by combining the PSO algorithm, position updating equations of the SCA, and the Lévy flight approach. The proposed method was shown to be very effective for tackling 23 benchmark functions, and 8 constrained real problems in engineering. Nenavath and Jatoth [63] developed the SCA-DE, an enhanced version of the SCA created by merging it with the Differential Evolution algorithm (DE). They verified the capabilities of the SCA-DE by using it to solve the 23 benchmark functions and object tracking cases. Their experimental results showed that the SCA-DE model outperformed the other hybrid approaches. Soon after that, Nenavath *et al*. [64] also developed a hybrid approach, which combined the SCA and PSO for object tracking cases. An improved SCA for tuning the forecast engine of air pollutant concentration was proposed by Li *et al*. [65], and their results demonstrated that the developed method could commendably accomplish the optimization process. Rizk-Allah [66] presented a new, improved version of the SCA that regarded a multi-orthogonal search strategy as a mechanism for solving engineering design problems and experimentally showed that the enhanced approach could produce very competitive results in most cases.

Additionally, Rizk-Allah [67] also proposed a hybrid optimization algorithm taking into account the combination of the orthogonal parallel information and SCA for solving numerical optimization problems and showed that it could reach a very high level of competition. A novel SCA using a Q-learning algorithm, Lévy flight motion, and a crossover strategy was proposed by Zamli *et al*. [68] to facilitate jumping out of local minima. Their experimental results indicated that the proposed algorithm outperformed other recent state-of-the-art strategies. Zhang *et al.* [69] hybridized the water wave optimization algorithm and SCA with elite opposition-based learning to deal with optimization functions and structural engineering design problems. The results confirmed that the developed algorithm could achieve a highly competitive performance compared with its peers, especially in convergence speed and calculation accuracy.

Motivated by these observations, an improved SCA variant, termed the CLSCA, using two strategies has been proposed. First, the Lévy flight with long jumps was well capable of increasing the diversity of the population. Then, the chaotic local search (CLS) strategy was added into the exploitation phase of the SCA to modify the exploitation searching process. To assess the performance of the improved CLSCA, its performance was compared with other well-known optimization methods, several variants of the SCA, and the well-known advanced algorithms in the literature. Nineteen classical benchmark functions and 30 CEC2014 benchmark functions with different characteristics have been utilized in this paper. The results showed that the proposed CLSCA method outperformed other optimization methods and the

state-of-the-art SCA variants in most benchmark cases. Different metrics and statistical validations provided evidence of the excellent performance of the proposed CLSCA in these experiments.

The organization of the paper is as follows. An overview of the SCA algorithm is shown in Section 2. The improved CLSCA is presented in Section 3. The experimental results are described and discussed in Section 4. Section 5 analyzes the experimental results of CLSCA on engineering problems. In section 6, the conclusions are drawn, and future works are summarized.

II. AN OVERVIEW OF SINE COSINE ALGORITHM (SCA)

The SCA is a new population-based optimization algorithm recently put forward by Mirjalili [51]. Like all the other stochastic optimization algorithms, the SCA process can be divided into two parts, namely the exploration phase and the exploitation phase [70]. Based on these two phases, different regions of the search space can be explored utilizing equations that include sine and cosine functions. The position updating equations are stated as follows:

$$X_{(i,j)}^{t+1} = X_{(i,j)}^{t} + rand_1 \times \sin(rand_2) \times \left| rand_3 DP_j^t - X_{(i,j)}^{t} \right| \quad (1)$$

$$X_{(i,j)}^{t+1} = X_{(i,j)}^{t} + rand_1 \times \cos(rand_2) \times \left| rand_3 DP_j^t - X_{(i,j)}^{t} \right| \quad (2)$$

where $X_{(i,j)}^{t}$ and $X_{(i,j)}^{t+1}$ are the positions of the i-th current search point in the j-th dimension at iterations of t and $t+1$, respectively; DP_j^t is the solution of the destination point in the j-th dimension, and $|\cdot|$ represents the absolute value; parameters $rand_1$, $rand_2$ and $rand_3$ are random parameters of the SCA. By combining these two equations, a new equation is constructed:

$$X_{(i,j)}^{t+1} = \begin{cases} X_{(i,j)}^{t} + rand_1 \times \sin(rand_2) \times \left| rand_3 DP_j^t - X_{(i,j)}^{t} \right|, & rand_4 < 0.5 \\ X_{(i,j)}^{t} + rand_1 \times \cos(rand_2) \times \left| rand_3 DP_j^t - X_{(i,j)}^{t} \right|, & rand_4 \geq 0.5 \end{cases} \quad (3)$$

where $rand_4 \in [0, 1]$ represents a random value and switches the sine and cosine components in Eq. (3). The parameters $rand_1$, $rand_2$, $rand_3$ and $rand_4$ are the four main primary parameters that influence the searching process of the SCA. The main task of $rand_1$ in Eq. (4) is to define the next position of the current search point that can be located in the space between the solution and destination point ($rand_1 < 1$) or outside it ($rand_1 > 1$).

$$rand_1 = A - tA/T \quad (4)$$

where constant A is set to 2, t indicates the current iteration, and T represents the maximum number of iterations. The parameter $rand_2 \in [0, 2\pi]$ defines how far the solution can be close to or far away from the destination point.

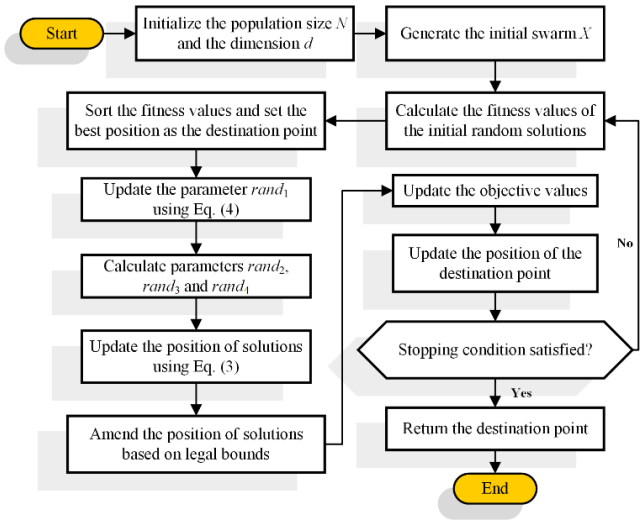

FIGURE 1. Flowchart of the SCA.

The function of $rand_3 \in [0, 2]$ is to control the effect of DP on the distance definition. The flowchart of the SCA is depicted in Figure 1.

III. PROPOSED CLSCA STRATEGY

The main purpose of this work is to improve the performance of the original SCA by combining it with the CLS strategy and the Lévy flight operator on the complex optimization problems. The Lévy flight operator is used to add the population diversity for the SCA, while the CLS strategy forces the solution to move towards the destination point in the exploitation phase. These two mechanisms also effectively balance exploration and exploitation abilities.

A. CHAOTIC LOCAL SEARCH

To further enhance the search performance of the method, the CLS strategy is embedded in the searching process of the SCA. Chaos is a typical non-linear phenomenon; it is ergodic, random, and sensitive to its initial conditions [71]. The primary function of the CLS strategy is to generate chaotic variables by a chaotic system. Chaos is also characterized by ergodicity and randomicity. Therefore, the chaotic regional search strategy conducts the second search in the neighborhood of the best search individual (destination point). The candidate solution of the destination point in the CLS method is generated *as* follows:

$$CS = (1 - \beth) \times DP + \beth \times CH_i' \quad i = 1, \cdots, N \quad (5)$$

where CS denotes the candidate solution, DP is the location of the best search individual, $\beth = (G - t+1)/G$ represents the contraction factor, and CH_i' is defined as follows:

$$CH_i' = lb + CH_i \times (ub - lb) \quad (6)$$

where lb and ub are, respectively, the lower and upper limits of the search space, CH_i' is a chaotic vector and CH_i is the

chaotic variable. The classic logistic map was used in this work, as shown in Eq. (7):

$$CH_i = \beta \times ch_i \times (1 - ch_i)\, i = 1, \cdots, N-1 \tag{7}$$

where we set $0 < ch_1 < 1$ and $ch_1 \neq 0.25, 0.5, 0.75, 1$; N is the number of searching individuals; $0 < \beta \leq 4$ is a chaotic attractor. In particular, when β is set to 4, the above classical logistic chaotic sequence is given as:

$$CH_i = 4ch_i \times (1 - ch_i)\, i = 1, \cdots, N-1 \tag{8}$$

B. LÉVY FLIGHT

The Lévy flight [39] has been employed in the SCA to enhance the search capabilities of the current search agents. The random number generated by the Lévy flight consists of the following two steps: the random selection of the direction and the generation of the step length values, which are based on the Lévy distribution rule. A simple version of Lévy distribution can be given as follows:

$$L(s, \gamma, \mu) = \begin{cases} \sqrt{\frac{\gamma}{2\pi}} exp\left[-\frac{\gamma}{2(s-\mu)}\right] \frac{1}{(s-\mu)^{3/2}}, & 0 < \mu < s < \infty \\ 0, & s \leq 0 \end{cases} \tag{9}$$

where μ denotes the location or shift parameter, and $\gamma > 0$ is a scale (controls the level of distribution) factor. Lévy distribution should be described in the light of Fourier transform.

$$F(k) = exp\left[-\alpha |k|^{\beta}\right], \quad 0 < \beta \leq 2 \tag{10}$$

where α is a parameter between $[-1, 1]$ and known as a scale factor, β is an index of stability. To obtain a deeper trade-off between the inclusive exploratory and neighborhood-informed capacities of the algorithm, the Lévy flight strategy can be used to update the location of the searched individual, which can be calculated as follows:

$$X_i^L = X_i + L(\delta) \oplus X_i \tag{11}$$

After the Lévy flight operator is complete, X_i^L is the new position of i-th individualX_i and $\oplus$ indicates the entry-wise multiplications.

C. CLSCA METHOD

Our proposed CLSCA combines two mechanisms. First, the chaotic local search strategy is introduced into the SCA to overcome the deficiency of stagnation in local optima. Then, to ensure the diversity of the population, the Lévy flight operator is employed in the updating process of the search agents. Here, the proposed CLSCA will be described in detail.

Step 1: The Lévy flight operation acts on the updating process of the current search individual to generate the new version of the search agent X_i^L according to Eq. (11). To ensure the quality of the CLSCA population, search individuals with higher fitness will be retained, which is generated as follows:

$$X_i^{t+1} = \begin{cases} X_i^L & fitness\left(X_i^L\right) > fitness(X_i) \\ X_i & otherwise \end{cases} \tag{12}$$

Step 2: The solution is generated by CLS strategy, and the location of the destination point in the whole searching process is updated. The modified mathematical model can be produced by:

$$DP^{t+1} = (1 - \propto) \times DP^t + \propto \times CH_i^{'} \tag{13}$$

where DP^t denotes the destination point during t generations and DP^{t+1} is the new version of the destination point in the $t+1$ iteration. It should be noted that the fittest version of DP can be stored in DP^{t+1} according to the CLS mechanism, then the quality of the destination point can be enhanced. Thus, problems of low diversity and stagnation in the local optima will be relieved. Accordingly, a suitable balance between exploration and exploitation can be kept in the CLSCA. The pseudo-code of the proposed CLSCA is represented as follows:

Algorithm 1 The pseudo-code of the CLSCA

```
Initialize the population X_i(i = 1, 2, ..., N)
Calculate the fitness values of the initial search individuals
Set the DP as the destination point
    while t< G
     Update rand_1 by Eq. (4)
     for i = 1: N
       for j = 1:d
            Calculate the parameters rand_2, rand_3 and
            rand_4
            Update the positions of the search agents
            by Eq. (3)
       End j
       Amend the position of the current search individual
       based on lb and ub
       Perform Lévy flight operator using Eq. (11)
       to generate a candidate search agent X_i^L
       Update the X_i^{t+1} by performing Eq. (12)
     End i
     Perform CLS strategy using Eq. (13) for DP
     Update DP if there is a better search individual
Return DP
```

The computational complexity of the improved CLSCA mainly depends on the total number of search agents (N), the number of algorithm iterations (G), and dimensions of the specific optimization tasks (d). The overall computational complexity of the proposed method is O(CLSCA)= O(*Initialize*)+O(*Calculate the fitness values of the initial search individuals*)+O(*Set DP*)+$G \times$ (O(*Update the current search agents*)+O(*Perform Lévy flight operator*)+O(*Update DP by CLS strategy*). Different optimization problems have different time complexities; thus, there is no O(*Calculate the fitness values*) consideration. The time complexity for initialization is $O(N \times d)$. Set the position of DP is $O(N^2)$. The computational complexity of updating all solutions is $O(G \times N \times d)$. Performing the Lévy flight operator for the swarm is $O(G \times (N \times d + N \times d + 4N))$.

TABLE 1. Description of the benchmark functions.

ID	Function Equation	*D*	*Range*	f_{min}
Unimodal Functions				
F1	$f_1(x)=\sum_{i=1}^{n}x_i^2$	30	[-100,100]	0
F2	$f_2(x)=\sum_{i=1}^{n}\lvert x_i\rvert+\prod_{i=1}^{n}\lvert x_i\rvert$	30	[-10,10]	0
F3	$f_3(x)=\sum_{i=1}^{n}(\sum_{j-1}^{i}x_j)^2$	30	[-100,100]	0
F4	$f_4(x)=max_i\{\lvert x_i\rvert,1\le i\le n\}$	30	[-100,100]	0
F5	$f_5(x)=\sum_{i=1}^{n-1}[100(x_{i+1}-x_i^2)^2+(x_i-1)^2]$	30	[-30,30]	0
F6	$f_6(x)=\sum_{i=1}^{n}([x_i+0.5])^2$	30	[-100,100]	0
F7	$f_7(x)=\sum_{i=1}^{n}ix_i^4+random[0,1)$	30	[-1.28,1.28]	0
Multimodal Functions				
F8	$f_8(x)=\sum_{i=1}^{n}-x_i\sin(\sqrt{\lvert x_i\rvert})$	30	[-500,500]	- 418.9829×5
F9	$f_9(x)=\sum_{i=1}^{n}[x_i^2-10\cos(2\pi x_i)+10]$	30	[-5.12,5.12]	0
F10	$f_{10}(x)=-20\exp\left\{-0.2\sqrt{\frac{1}{n}\sum_{i=1}^{n}x_i}\right\}-exp\{\frac{1}{n}\sum_{i=1}^{n}\cos(2\pi x_i)\}+20+e$	30	[-32,32]	0
F11	$f_{11}(x)=\frac{1}{4000}\sum_{i=1}^{n}x_i^2-\prod_{i=1}^{n}\cos\left(\frac{x_i}{\sqrt{i}}\right)+1$	30	[-600,600]	0
F12	$f_{12}(x)=\frac{\pi}{n}\{10\sin(ay_1)+\sum_{i=1}^{n-1}(y_i-1)^2[1+10sin^2(\pi y_{i+1})]+(y_n-1)^2+\sum_{i=1}^{n}\mu(x_i,10,100,4)\}$ $y_i=1+\frac{x_i+1}{4}$ $\mu(x_i,a,k,m)=\begin{cases}k(x_i-a)^m & x_i>a\\ 0 & -a<x_i<a\\ k(-x_i-a)^m & x_i<-a\end{cases}$	30	[-50,50]	0
F13	$f_{13}(x)=0.1\{sin^2(3\pi x_i)+\sum_{i=1}^{n}(x_i-1)^2[1+sin^2(3\pi x_i+1)]+(x_n-1)^2[1+sin^2(2\pi x_n)]+\sum_{i=1}^{n}\mu(x_i,5,100,4)$	30	[-50,50]	0
Fixed-dimension multimodal Functions				
F14	$f_{14}(x)=\left(\frac{1}{500}+\sum_{j=1}^{25}\frac{1}{j+\sum_{i=1}^{2}(x_i-a_{ij})^6}\right)^{-1}$	2	[-65,65]	1
F15	$f_{15}(x)=\sum_{i=1}^{11}\left[a_i-\frac{x_1(b_i^2-b_ix_2)}{b_i^2+b_ix_3+x_4}\right]^2$	4	[-5,5]	0.00030
F16	$f_{16}(x)=[1+(x_1+x_2+1)^2(19-14x_1+3x_1^2-14x_2+6x_1x_2+3x_2^2)]\times[30+(2x_1-3x_2)^2(18-32x_1+12x_1^2+48x_2-36x_1x_2+27x_2^2)]$	2	[-2,2]	3
F17	$f_{17}(x)=-\sum_{i=1}^{5}[(X-a_i)(X-a_i)^T+c_i]^{-1}$	4	[0,10]	-10.1532
F18	$f_{18}(x)=-\sum_{i=1}^{7}[(X-a_i)(X-a_i)^T+c_i]^{-1}$	4	[0,10]	-10.4028
F19	$f_{19}(x)=-\sum_{i=1}^{10}[(X-a_i)(X-a_i)^T+c_i]^{-1}$	4	[0,10]	-10.5363
CEC 2014 Composition Functions				
F20	Shifted and Rotated Bent Cigar Function	30	[-100,100]	100
F21	Shifted and Rotated Sum of Different Power Function	30	[-100,100]	200
F22	Shifted and Rotated Zakharov Function	30	[-100,100]	300
F23	Shifted and Rotated Rosenbrock's Function	30	[-100,100]	400
F24	Shifted and Rotated Rastrigin's Function	30	[-100,100]	500
F25	Shifted and Rotated Expanded Scaffer's F6 Function	30	[-100,100]	600
F26	Shifted and Rotated Lunacek Bi-Rastrigin Function	30	[-100,100]	700
F27	Shifted and Rotated Non-Continuous Rastrigin's Function	30	[-100,100]	800
F28	Shifted and Rotated Lévy Function	30	[-100,100]	900
F29	Shifted and Rotated Schwefel's Function	30	[-100,100]	1000

TABLE 1. *(Continued.)* Description of the benchmark functions.

F30	Hybrid Function 1 (N=3)	30	[-100,100]	1100
F31	Hybrid Function 2 (N=3)	30	[-100,100]	1200
F32	Hybrid Function 3 (N=3)	30	[-100,100]	1300
F33	Hybrid Function 4 (N=4)	30	[-100,100]	1400
F34	Hybrid Function 5 (N=4)	30	[-100,100]	1500
F35	Hybrid Function 6 (N=4)	30	[-100,100]	1600
F36	Hybrid Function 6 (N=5)	30	[-100,100]	1700
F37	Hybrid Function 6 (N=5)	30	[-100,100]	1800
F38	Hybrid Function 6 (N=5)	30	[-100,100]	1900
F39	Hybrid Function 6 (N=6)	30	[-100,100]	2000
F40	Composition Function 1 (N=3)	30	[-100,100]	2100
F41	Composition Function 2 (N=3)	30	[-100,100]	2200
F42	Composition Function 3 (N=4)	30	[-100,100]	2300
F43	Composition Function 4 (N=4)	30	[-100,100]	2400
F44	Composition Function 5 (N=5)	30	[-100,100]	2500
F45	Composition Function 6 (N=5)	30	[-100,100]	2600
F46	Composition Function 7 (N=6)	30	[-100,100]	2700
F47	Composition Function 8 (N=6)	30	[-100,100]	2800
F48	Composition Function 9 (N=3)	30	[-100,100]	2900
F49	Composition Function 10 (N=3)	30	[-100,100]	3000

The time complexity of $O(Updating\ DP)$ by CLS strategy is $O(G\times(N\times d+N\times d+N^2))$. Therefore, the time complexity of the proposed CLSCA is as follows:

$$\begin{aligned} O(\text{CLSCA}) &= O(N\times d)+O(N^2)+G\times(N\times d+N\times d \\ &\quad +N\times d+4N+N\times d+N\times d+N^2) \\ &= O(N\times d+N^2)+G\times(5O(N\times d) \\ &\quad +4O(N)+O(N^2)). \end{aligned} \tag{14}$$

IV. EXPERIMENTAL RESULTS AND DISCUSSION

A. BENCHMARK FUNCTION VALIDATION

Through this experiment, we selected 49 benchmark functions to compare the proposed CLSSCA with other competitive algorithms. These include unimodal functions, multimodal functions, fixed-dimension multimodal functions, hybrid functions, and composition functions (See F1-F49). Here, 19 benchmark functions are classic test functions chosen from an earlier study [72]. F20-F49 functions are selected from IEEE CEC2014 benchmark functions [73]. The 49 benchmark functions are described in detail in Table 1, where D and $Range$ are the dimensions of the corresponding function and the boundary of the search space, respectively, and $f_{\min}$ represents the optimal value.

For unbiased experimental results, experiments were conducted under the same conditions, to reduce the impact of randomness; each benchmark function was independently performed 30 times in different tests.

B. THE IMPACT OF CLS AND LF STRATEGY

The improved CLSCA introduces two strategies into the original SCA, namely the CLS and Lévy flight. As shown in Table 2, we investigated the effects of each of the three different SCA variant tests on the proposed algorithm. In Table 2, "CLS" and "LF" denote "Chaotic local search" and "Lévy flight", respectively. Also, in Table 2, "1" indicates that the method is added to the algorithm, while "0" shows that the method is not added. For example, LSCA means that the SCA combines "LF" without "CLS".

TABLE 2. Various SCA variants with three strategies.

	CLS	LF
SCA	0	0
LSCA	0	1
CSCA	1	0
CLSCA	1	1

In this section, 26 benchmark functions, including unimodal functions, multimodal functions, fixed-dimension multimodal functions, and composition functions, are selected. Also, for the validation of the experimental results, each algorithm was tested under the same parameter settings. The Friedman test [74] can rank the average of the performance of these methods to establish the differences between them. According to Table 3, the CLSCA method has the lowest ranking value; thus, the CLSCA performs best in the 26 benchmark functions compared to the other methods. From the above analysis, the combination of CLS and Lévy flight is the best way to improve the SCA, which also proves the effectiveness of our improved algorithm CLSCA.

Figure 2 shows the change of solution and adaptation values of CLSCA and its variants. On F7, Figure 2. (a) shows the solution spatial distribution of CLSCA, and it can be clearly

TABLE 3. Average ranking values of various SCA variants using the Friedman test.

Function	metric	CLSCA	LSCA	CSCA	SCA
F1	mean	0.00E+00	0.00E+00	2.32E-10	4.70E-52
	std.	0.00E+00	0.00E+00	1.10E-09	2.57E-51
F2	mean	0.00E+00	0.00E+00	1.26E-23	5.60E-60
	std.	0.00E+00	0.00E+00	5.66E-23	2.30E-59
F3	mean	0.00E+00	0.00E+00	6.65E-04	2.86E+00
	std.	0.00E+00	0.00E+00	2.63E-03	7.31E+00
F4	mean	0.00E+00	0.00E+00	1.74E-05	1.41E-02
	std.	0.00E+00	0.00E+00	1.46E-05	4.61E-02
F5	mean	7.19E-08	2.79E+01	1.00E-07	2.70E+01
	std.	1.34E-07	7.07E-01	1.21E-07	3.98E-01
F6	mean	1.01E-08	4.30E+00	7.58E-09	3.61E+00
	std.	1.43E-08	2.47E-01	1.29E-08	2.58E-01
F7	mean	5.12E-05	5.16E-05	1.24E-04	2.63E-03
	std.	4.59E-05	5.45E-05	1.23E-04	1.79E-03
F8	mean	-1.26E+04	-5.13E+03	-1.26E+04	-4.37E+03
	std.	1.39E-07	6.31E+02	7.69E-07	2.16E+02
F9	mean	0.00E+00	0.00E+00	5.28E-09	8.55E-09
	std.	0.00E+00	0.00E+00	2.51E-08	4.68E-08
F10	mean	8.88E-16	8.88E-16	2.53E-06	7.09E+00
	std.	0.00E+00	0.00E+00	7.42E-06	8.65E+00
F11	mean	0.00E+00	0.00E+00	1.85E-17	2.04E-05
	std.	0.00E+00	0.00E+00	1.01E-16	1.12E-04
F12	mean	4.96E-11	4.32E-01	8.96E-11	3.34E-01
	std.	7.53E-11	4.67E-02	1.28E-10	5.06E-02
F13	mean	1.59E-08	2.32E+00	1.03E-09	1.97E+00
	std.	7.87E-08	1.14E-01	1.54E-09	1.62E-01
F14	mean	9.98E-01	2.05E+00	9.98E-01	9.98E-01
	std.	1.45E-13	1.91E+00	1.52E-15	4.82E-07
F15	mean	3.23E-04	3.22E-04	3.24E-04	5.59E-04
	std.	2.79E-05	7.19E-06	1.30E-05	4.01E-04
F16	mean	3.00E+00	3.00E+00	3.00E+00	3.00E+00
	std.	1.85E-07	1.29E-07	7.09E-07	1.59E-07
F17	mean	-1.02E+01	-3.93E+00	-1.02E+01	-2.61E+00
	std.	3.40E-10	2.32E+00	5.24E-10	2.37E+00
F18	mean	-1.04E+01	-4.21E+00	-1.04E+01	-4.16E+00
	std.	4.40E-10	1.98E+00	4.85E-10	2.59E+00
F19	mean	-1.05E+01	-5.28E+00	-1.05E+01	-5.65E+00
	std.	4.03E-10	1.56E+00	4.49E-10	2.82E+00
F42	mean	2.50E+03	2.50E+03	2.50E+03	2.67E+03
	std.	0.00E+00	0.00E+00	8.63E-04	1.47E+01
F43	mean	2.60E+03	2.60E+03	2.60E+03	2.60E+03
	std.	0.00E+00	0.00E+00	4.82E-02	1.33E-01
F44	mean	2.70E+03	2.70E+03	2.70E+03	2.73E+03
	std.	0.00E+00	0.00E+00	1.11E-04	6.55E+00
F46	mean	2.90E+03	2.90E+03	2.90E+03	3.44E+03
	std.	0.00E+00	0.00E+00	7.88E-07	3.29E+02
F47	mean	3.00E+03	3.00E+03	3.00E+03	4.89E+03
	std.	0.00E+00	0.00E+00	3.68E-03	4.03E+02
F48	mean	3.10E+03	3.10E+03	6.86E+03	1.29E+07
	std.	0.00E+00	0.00E+00	1.75E+04	7.34E+06
F49	mean	3.20E+03	3.20E+03	1.08E+05	2.49E+05
	std.	0.00E+00	0.00E+00	1.40E+05	7.04E+04
	Ranking	1.645513	2.427564	2.519231	3.407692

seen that most of the solution positions are concentrated around the optimal solution. Figure 2. (b) shows the distribution of solutions in the first dimension. It can be seen that the solution of CLSCA shrinks faster than other SCA variants and has a strong anti-interference ability. Figure 2. (c) shows the change in the average fitness value. It is obvious that

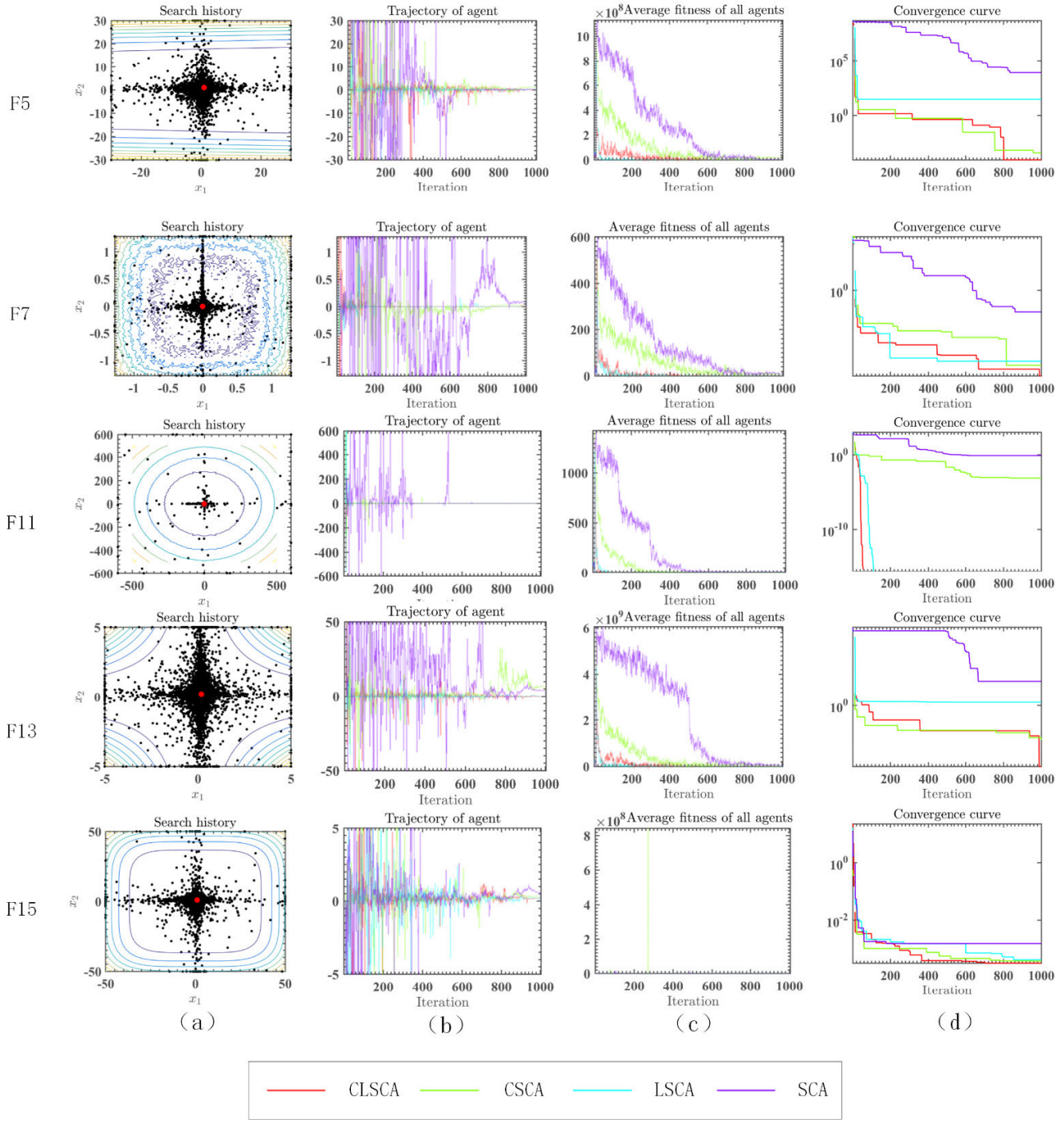

FIGURE 2. (a) Location distribution of CLSCA on several benchmark functions, (b) Trajectory of SCA variants in the first dimension, (c) Average fitness of SCA variants, (d) Convergence curves of SCA variants.

CLSCA converges faster than CSCA and SCA in the early stage. Figure 2. (d) shows the change of the optimal value, and CLSCA achieves the optimal solution faster than other SCA variants. In general, CLSCA is superior to other SCA variants in all graphs.

C. SCALABILITY TEST

To further test the performance of the CLSCA, the scalability was tested by comparing the results of the CLSCA with those of the original SCA in different dimensions. The optimization algorithm evaluates the impact of dimensions on its effectiveness through scalability tests. The influence of increasing the dimension on the CLSCA solution is evaluated. The experiment explored four different dimensions, namely 100, 500, 1000, and 2000. In the test, the number of evaluations and population size was set as 1000000 and 30, respectively. Also, each method is independently executed 30 times. The average optimal value (mean) and standard deviation (std) of the

TABLE 4. Comparison results of the different dimensions.

Fun	Method	*D*=100		*D*=500		*D*=1000		*D*=20000	
		mean	std	mean	std	mean	std	mean	std
F1	CLSCA	0.00E+00	0.00E+00	0.00E+00	0.00E+00	0.00E+00	0.00E+00	0.00E+00	0.00E+00
	SCA	1.97E-01	1.02E+00	7.59E+04	3.28E+04	2.60E+05	7.98E+04	6.15E+05	1.54E+05
F2	CLSCA	0.00E+00	0.00E+00	0.00E+00	0.00E+00	0.00E+00	0.00E+00	0.00E+00	0.00E+00
	SCA	1.88E-42	8.95E-42	2.81E+01	2.67E+01	6.55E+04	7.62E+01	6.55E+04	3.72E+02
F3	CLSCA	0.00E+00	0.00E+00	0.00E+00	0.00E+00	0.00E+00	0.00E+00	0.00E+00	0.00E+00
	SCA	7.71E+04	1.83E+04	2.91E+06	4.31E+05	1.23E+07	1.55E+06	5.14E+07	6.89E+06
F4	CLSCA	0.00E+00	0.00E+00	0.00E+00	0.00E+00	0.00E+00	0.00E+00	0.00E+00	0.00E+00
	SCA	5.53E+01	7.32E+00	9.62E+01	6.58E-01	9.87E+01	1.89E-01	9.95E+01	9.55E-02
F5	CLSCA	2.58E-06	5.01E-06	3.03E-05	5.10E-05	1.47E-05	2.15E-05	3.25E-05	7.15E-05
	SCA	1.93E+05	3.91E+05	5.82E+08	1.76E+08	2.08E+09	3.05E+08	4.81E+09	8.24E+08
F6	CLSCA	3.03E-07	6.07E-07	1.55E-06	2.16E-06	6.73E-06	1.36E-05	4.25E-06	6.35E-06
	SCA	2.21E+01	2.37E+00	7.00E+04	2.69E+04	2.52E+05	7.88E+04	6.26E+05	1.81E+05
F7	CLSCA	1.81E-05	1.48E-05	2.50E-05	2.53E-05	1.58E-05	1.31E-05	1.78E-05	2.10E-05
	SCA	6.05E-01	6.39E-01	4.71E+03	1.04E+03	2.75E+04	5.24E+03	1.38E+05	3.05E+04
F8	CLSCA	-4.19E+04	3.09E-07	-2.09E+05	1.17E-06	-4.19E+05	6.71E-06	-8.38E+05	1.19E-05
	SCA	-8.64E+03	3.65E+02	-1.95E+04	1.08E+03	-2.70E+04	1.52E+03	-3.89E+04	2.02E+03
F9	CLSCA	0.00E+00	0.00E+00	0.00E+00	0.00E+00	0.00E+00	0.00E+00	0.00E+00	0.00E+00
	SCA	5.78E+01	5.78E+01	9.01E+02	3.65E+02	1.46E+03	7.78E+02	2.96E+03	1.79E+03
F10	CLSCA	8.88E-16	0.00E+00	8.88E-16	0.00E+00	8.88E-16	0.00E+00	8.88E-16	0.00E+00
	SCA	1.76E+01	7.06E+00	1.97E+01	3.28E+00	1.60E+01	5.67E+00	1.77E+01	4.95E+00
F11	CLSCA	0.00E+00	0.00E+00	0.00E+00	0.00E+00	0.00E+00	0.00E+00	0.00E+00	0.00E+00
	SCA	1.07E-01	2.30E-01	6.92E+02	2.09E+02	2.06E+03	6.54E+02	5.11E+03	1.20E+03
F12	CLSCA	3.43E-10	5.94E-10	1.75E-10	2.67E-10	1.61E-10	2.93E-10	9.55E-11	1.75E-10
	SCA	1.99E+05	3.45E+05	1.58E+09	3.50E+08	4.93E+09	8.91E+08	1.28E+10	1.58E+09
F13	CLSCA	1.06E-08	1.65E-08	3.93E-08	6.57E-08	7.46E-08	1.34E-07	2.28E-07	4.04E-07
	SCA	9.88E+05	1.95E+06	2.93E+09	5.20E+08	8.68E+09	1.22E+09	2.20E+10	3.71E+09

algorithm under multiple dimensions are shown in Table 4. The data in Table 4 reveals that, in high-dimensional experiments, the optimal value of the convergence of the CLSCA is still higher than that of the SCA. At the same time, since the high-dimensional problem is more challenging to address, the standard deviation of the high-dimensional problem increases with the increase of the dimension. Therefore, the CLSCA can offer better results in all functions from F1 to F13.

D. COMPARISON OF CLSCA WITH CLASSICAL METAHEURISTIC ALGORITHMS

In this section, we compare the improved CLSCA with eight successful metaheuristic algorithms, including SCA, GWO, WOA, MFO, BA [22], gravitational search algorithm (GSA) [75], firefly algorithm (FA) and PSO. In the experiment, we set the number of evaluations as 300,000, the population size as 30 times, and the dimension of the search space as 30. The main parameter settings for all compared algorithms are shown in Table 5. In addition, 26 functions mentioned above have been utilized in this part. The results of the comparison of the CLSCA with other algorithms are shown in Table 6; they include the mean and std of the 26 functions after 30 independent executions. Additionally, Table 6 also shows the Friedman test used to check the average ranking. The statistical comparison results of the Wilcoxon test [76] are shown in Table 7. The P values for the CLSCA and other compared algorithms shown in Table 7 reveal, as indicated by the symbols "+", "-" and "=" in the last line of the table, that the CLSCA was better, worse or equal in performance to the corresponding algorithm.

The test results of the CLSCA and other competing methods in the 26 functions are listed in Table 6. The average result of the CLSCA is better than those of its competitors on most tasks. The Friedman test was also applied to sort the average performance of the algorithms. The ranking reveals that the

TABLE 5. Parameters setting for algorithms.

Method	Population size	Maximum evaluation times	Other parameters
CLSCA	30	30,0000	$a = 2$; $r_2 \in [0\ 2\pi]$; $r_3 \in [0\ 2]$; $r_4 \in [0\ 1]$; μ=4; $C_1 \in [0\ 1]$ and $C_1 \neq$0,0.25,0.50,0.75,1.00
MFO	30	30,0000	b =1; $t \in$ [-1 1]; $a \in$ [-1 -2]
BA	30	30,0000	A = 0.5; r = 0.5; $\alpha = \gamma$ = 0.9
SCA	30	30,0000	$a = 2$; $r_2 \in [0\ 2\pi]$; $r_3 \in [0\ 2]$; $r_4 \in [0\ 1]$
PSO	30	30,0000	c_1= 2; c_2 = 2; v_{max}= 6
WOA	30	30,0000	$a_1 \in [2\ 0]$; $a_2 \in$ [-2 -1]; b = 1
FA	30	30,0000	β_0=1; $\alpha \in [0\ 1]$; γ = 1
GSA	30	30,0000	α=20; G_0=100
GWO	30	30,0000	$a \in$ [2,0]; $r_1 \in [0\ 1]$; $r_2 \in [0\ 1]$

CLSCA is superior to other algorithms. The CLSCA not only improves the performance of the original SCA but also outperforms different algorithms. Also, the CLSCA has the smallest std compared to other algorithms, indicating that the CLSCA has restored stability, and the optimal solution found has the lowest error. The Friedman test was used to assess the average ranking value of the algorithm, as shown in the last row of Table 6. According to the ranking results, the average ranking of the CLSCA is the lowest among all the compared algorithms, indicating that it has better performance than the other algorithms. The data presented in Table 7 reveal that most P values obtained by the comparison of the algorithms are less than 0.05. Among the 26 compared functions, the "+/-/=" scores displayed by the CLSCA relative to the FA, BA, GSA, and PSO algorithms are all "26/0/0", respectively, while most of the other compared algorithms are also "+". These results show that the CLSCA has apparent advantages over the other algorithms, and has statistically significant better performance in unimodal functions, multimodal functions, fixed-dimension multimodal functions, and composition functions.

The convergence curves of six representative different benchmark problems are shown in Figure 3. The convergence curves show that the CLSCA has a better convergence trend in the late evaluation period when implementing the F5 and F13 problems. In the F7 and F10 issues, the CLSCA does not have faster convergence than that of the GWO in the early stage, but as the number of evaluations increases, the convergence accuracy of the CLSCA is higher than that of all competitors. F15 and F49 are also higher in terms of the solution quality than all other competitors. In six problems, the CLSCA has a more top convergence speed than all its competitors.

E. WALL-CLOCK TIME COST

The wall-clock time required by CLSCA and the other 8 optimizers on 26 tasks mentioned above are shown in Table 8. We have recorded the wall-clock time over 30 independent runs. With regard to wall-clock time for all 26 problems, it can be decided that the suggested CLSCA consumes only a short time than basic SCA. The leading causes for the occurrence of the said phenomena are that two strategies (CLS strategy and Lévy flight operator) are introduced in the conventional SCA to achieve a better balance between the exploratory and exploitative properties. Overall, it is observed that the wall-clock time budget of the conventional WOA, GSA, BA, and FA is much higher than that of CLSCA in 26 benchmark functions. Although the time-consuming of the proposed technique is higher than that of basic SCA, MFO, GWO, and PSO, it can be found from the obtained experimental results that CLSCA is significantly better than the original SCA and other peers in most functions. Therefore, it is very feasible to embed two synchronizing policies into the SCA.

F. COMPARISION WITH ADVANCED ALGORITHMS

Apart from some of the traditional methods tested, we also added five advanced algorithms, namely, SCA with differential evolution (SCADE) [63], opposition-based SCA (OBSCA) [57], fuzzy self-tuning PSO (FST_PSO) [77], chaotic SSA (CSSA) [78] and chaotic whale optimizer (CWOA) [79], to further evaluate the efficacy of the CLSCA. For comparison purposes, 13 benchmarks mentioned above (F1-F13) with two unimodal and multi-modal multimodal functions are chosen from 23 common benchmark cases. Also, 30 CEC2014 benchmark tests (F20-F49) are chosen for further evaluate the performance of the CLSCA. In this part, the number of evaluations and the population size were set as 450,000 and 30, respectively. The parameters of the above algorithms are set according to their settings in the original paper in which they were reported. The main parameter settings of each algorithm in the experiment are shown in Table 9. The parameters for the dimensions, number of evaluations, and population size in the experiment are set as described in Section 4.4.

TABLE 6. Comparison results of CLSCA and other algorithms.

Function	metric	CLSCA	WOA	GWO	MFO	BA	GSA	SCA	FA	PSO
F1	mean	0.00E+00	0.00E+00	0.00E+00	1.33E+03	6.33E-01	1.50E+01	1.37E-55	1.13E+04	1.02E+02
	std.	0.00E+00	0.00E+00	0.00E+00	3.46E+03	4.19E-01	1.39E+00	6.75E-55	8.67E+02	9.73E+00
F2	mean	0.00E+00	0.00E+00	0.00E+00	2.70E+01	5.79E+01	1.55E+01	1.85E-56	4.85E+01	4.76E+01
	std.	0.00E+00	0.00E+00	0.00E+00	1.88E+01	2.97E+02	8.69E-01	1.01E-55	3.39E+00	3.90E+00
F3	mean	0.00E+00	3.31E+01	4.12E-182	1.52E+04	3.05E-01	2.95E+02	1.18E+01	1.94E+04	1.80E+02
	std.	0.00E+00	5.00E+01	0.00E+00	1.17E+04	2.75E-01	6.26E+01	6.26E+01	2.17E+03	2.49E+01
F4	mean	0.00E+00	5.29E+00	5.29E-152	6.62E+01	4.04E+00	1.76E+00	3.00E-02	3.95E+01	3.80E+00
	std.	0.00E+00	1.17E+01	4.25E-05	8.24E+00	4.48E+00	1.19E-01	1.25E-01	3.25E+00	2.51E-01
F5	mean	3.59E-07	2.43E+01	2.63E+01	1.85E+04	2.99E+02	8.77E+03	2.73E+01	7.11E+06	8.61E+04
	std.	1.32E-06	3.92E-01	8.82E-01	3.64E+04	3.71E+02	2.50E+03	7.53E-01	1.44E+06	1.74E+04
F6	mean	1.14E-08	5.14E-06	4.21E-01	4.67E+03	6.40E-01	1.49E+01	3.63E+00	1.17E+04	9.91E+01
	std.	2.01E-08	1.98E-06	2.47E-01	6.81E+03	3.52E-01	2.06E+00	2.72E-01	9.82E+02	1.27E+01
F7	mean	4.89E-05	1.12E-04	6.77E-05	5.72E+00	1.36E+01	3.17E+01	2.27E-03	3.95E+00	1.07E+02
	std.	3.59E-05	1.66E-04	4.25E-05	1.08E+01	8.20E+00	3.94E+00	2.28E-03	9.22E-01	2.16E+01
F8	mean	-1.26E+04	-1.25E+04	-6.16E+03	-8.38E+03	-7.14E+03	-2.49E+03	-4.38E+03	-4.14E+03	-6.62E+03
	std.	1.07E-06	2.76E+02	8.35E+02	1.09E+03	8.48E+02	3.59E+02	2.99E+02	2.63E+02	8.67E+02
F9	mean	0.00E+00	0.00E+00	0.00E+00	1.50E+02	2.51E+02	1.98E+02	0.00E+00	2.30E+02	3.46E+02
	std.	0.00E+00	0.00E+00	0.00E+00	4.30E+01	1.73E+01	8.93E+00	0.00E+00	9.81E+00	1.62E+01
F10	mean	8.88E-16	3.49E-15	7.76E-15	1.59E+01	3.26E+00	4.16E+00	1.21E+01	1.58E+01	7.69E+00
	std.	0.00E+00	1.60E-15	9.01E-16	7.26E+00	4.61E+00	1.75E-01	9.11E+00	4.60E-01	3.32E-01
F11	mean	0.00E+00	9.41E-04	0.00E+00	3.91E+01	1.79E-02	5.41E-01	1.53E-02	1.05E+02	1.02E+00
	std.	0.00E+00	5.15E-03	0.00E+00	5.13E+01	1.72E-02	4.59E-02	8.39E-02	8.41E+00	1.39E-02
F12	mean	5.76E-11	2.20E-04	5.00E-02	1.25E-01	9.55E+00	1.35E+00	3.29E-01	2.22E+06	3.49E+00
	std.	8.47E-11	1.20E-03	9.80E-02	3.83E-01	4.47E+00	2.78E-01	5.04E-02	1.02E+06	6.63E-01
F13	mean	8.82E-10	7.55E-04	4.01E-01	1.37E+07	1.56E-01	8.30E+00	1.94E+00	1.61E+07	1.53E+01
	std.	1.37E-09	2.79E-03	2.10E-01	7.49E+07	8.32E-02	9.24E-01	1.06E-01	4.61E+06	1.66E+00
F14	mean	9.98E-01	1.06E+00	4.78E+00	1.85E+00	3.36E+00	9.98E-01	9.98E-01	9.98E-01	3.33E+00
	std.	3.10E-15	3.62E-01	4.37E+00	1.57E+00	2.87E+00	3.27E-04	4.55E-07	2.06E-05	2.84E+00
F15	mean	3.19E-04	4.33E-04	3.02E-03	8.87E-04	5.49E-03	1.10E-03	5.98E-04	9.70E-04	9.68E-04
	std.	7.12E-06	2.81E-04	6.92E-03	5.43E-04	8.35E-03	2.20E-04	4.16E-04	1.73E-04	4.45E-05
F16	mean	3.00E+00	3.00E+00	3.00E+00	3.00E+00	3.01E+00	3.01E+00	3.00E+00	3.00E+00	3.01E+00
	std.	3.64E-07	7.45E-08	8.83E-08	1.99E-15	6.67E-03	6.12E-03	2.08E-07	1.53E-03	8.14E-03
F17	mean	-1.02E+01	-1.02E+01	-9.31E+00	-6.39E+00	-7.79E+00	-6.24E+00	-2.54E+00	-8.19E+00	-6.90E+00
	std.	3.05E-10	1.07E-06	1.92E+00	3.46E+00	2.22E+00	1.24E+00	2.31E+00	8.04E-01	1.66E+00
F18	mean	-1.04E+01	-1.04E+01	-1.00E+01	-7.45E+00	-8.73E+00	-7.03E+00	-3.90E+00	-8.47E+00	-7.74E+00
	std.	2.17E-10	9.19E-07	1.39E+00	3.26E+00	1.82E+00	1.53E+00	2.52E+00	9.12E-01	1.17E+00
F19	mean	-1.05E+01	-1.05E+01	-1.05E+01	-6.98E+00	-9.30E+00	-6.26E+00	-4.77E+00	-8.64E+00	-7.65E+00
	std.	2.17E-09	5.89E-06	1.41E-06	3.90E+00	1.22E+00	1.06E+00	2.69E+00	7.96E-01	1.25E+00
F42	mean	2.50E+03	2.63E+03	2.63E+03	2.67E+03	2.62E+03	2.61E+03	2.67E+03	2.74E+03	2.62E+03
	std.	0.00E+00	6.13E+00	7.54E+00	3.62E+01	2.50E-03	6.49E+00	1.37E+01	1.63E+01	4.06E-01
F43	mean	2.60E+03	2.61E+03	2.60E+03	2.68E+03	2.66E+03	2.61E+03	2.60E+03	2.70E+03	2.63E+03
	std.	0.00E+00	4.38E+00	6.47E-04	3.36E+01	2.55E+01	4.10E-01	6.08E-02	5.42E+00	5.17E+00
F44	mean	2.70E+03	2.72E+03	2.71E+03	2.72E+03	2.73E+03	2.70E+03	2.72E+03	2.73E+03	2.71E+03
	std.	0.00E+00	1.78E+01	4.77E+00	1.16E+01	1.49E+01	1.33E-01	1.11E+01	4.44E+00	6.65E+00
F46	mean	2.90E+03	3.66E+03	3.36E+03	3.69E+03	3.97E+03	3.19E+03	3.46E+03	3.80E+03	3.48E+03
	std.	0.00E+00	3.85E+02	9.64E+01	1.10E+02	3.65E+02	1.15E+02	3.14E+02	2.49E+01	2.71E+02
F47	mean	3.00E+03	5.06E+03	3.82E+03	3.91E+03	5.35E+03	4.73E+03	4.81E+03	4.21E+03	6.99E+03
	std.	0.00E+00	5.26E+02	1.06E+02	2.03E+02	6.52E+02	3.95E+02	3.12E+02	9.01E+01	9.96E+02
F48	mean	3.10E+03	5.64E+06	9.26E+05	3.51E+06	3.92E+07	4.05E+07	1.16E+07	3.41E+06	5.38E+04
	std.	0.00E+00	5.03E+06	2.00E+06	3.86E+06	3.89E+07	5.83E+07	7.32E+06	1.02E+06	1.09E+05
F49	mean	3.20E+03	6.04E+04	5.91E+04	3.82E+04	1.04E+04	7.84E+03	2.41E+05	1.72E+05	1.48E+04
	std.	0.00E+00	3.34E+04	5.11E+04	3.25E+04	4.07E+03	8.53E+02	1.07E+05	4.64E+04	5.83E+03
	Ranking	1.744872	3.405769	3.475	5.028846	5.838462	5.983333	5.514744	7.433333	6.575641

The mean and std values of the different algorithms with 30 independent tests are listed in Table 10. Specifically, Table 10 contains the mean and std of the CLSCA and five compared algorithms over the 43 testing functions. The average value of the CLSCA on most functions is less than the competing algorithm, and the std is within a small range. To more intuitively assess the advantages and disadvantages of the CLSCA and the compared algorithms,

TABLE 7. Results of the statistical comparison between CLSCA and other algorithms by the Wilcoxon test.

Function	FA	WOA	GWO	MFO	BA	GSA	SCA	PSO
F1	1.73E-06	1	1	1.72E-06	1.73E-06	1.73E-06	1.73E-06	1.73E-06
F2	1.73E-06	1	1	1.49E-06	1.73E-06	1.73E-06	1.73E-06	1.73E-06
F3	1.73E-06	1.73E-06	1.73E-06	1.73E-06	1.73E-06	1.73E-06	1.73E-06	1.73E-06
F4	1.73E-06	1.73E-06	1.73E-06	1.73E-06	1.73E-06	1.73E-06	1.73E-06	1.73E-06
F5	1.73E-06	1.73E-06	1.73E-06	1.73E-06	1.73E-06	1.73E-06	1.73E-06	1.73E-06
F6	1.73E-06	1.73E-06	1.73E-06	0.382034	1.73E-06	1.73E-06	1.73E-06	1.73E-06
F7	1.73E-06	0.120445	0.097772	1.73E-06	1.73E-06	1.73E-06	1.73E-06	1.73E-06
F8	1.73E-06	1.73E-06	1.73E-06	1.73E-06	1.73E-06	1.73E-06	1.73E-06	1.73E-06
F9	1.73E-06	1	1	1.73E-06	1.73E-06	1.73E-06	1	1.73E-06
F10	1.73E-06	2.73E-06	1.01E-07	1.72E-06	1.73E-06	1.73E-06	1.72E-06	1.73E-06
F11	1.73E-06	1	1	5.96E-05	1.73E-06	1.73E-06	0.5	1.73E-06
F12	1.73E-06	1.73E-06	1.73E-06	0.205888	1.73E-06	1.73E-06	1.73E-06	1.73E-06
F13	1.73E-06	1.73E-06	1.73E-06	0.000616	1.73E-06	1.73E-06	1.73E-06	1.73E-06
F14	1.73E-06	0.176501	1.73E-06	0.640181	1.73E-06	1.73E-06	1.73E-06	1.73E-06
F15	1.73E-06	0.926255	0.165027	0.000115	1.73E-06	1.73E-06	0.003854	1.73E-06
F16	1.73E-06	0.191522	0.360039	1.73E-06	1.73E-06	1.73E-06	0.011748	1.73E-06
F17	1.73E-06	0.152861	3.88E-06	0.003609	1.73E-06	1.73E-06	1.73E-06	1.73E-06
F18	1.73E-06	1.73E-06	0.000359	0.047162	1.73E-06	1.73E-06	1.73E-06	1.73E-06
F19	1.73E-06	1.73E-06	1.73E-06	0.047162	1.73E-06	1.73E-06	1.73E-06	1.73E-06
F42	1.73E-06	1.73E-06	1.73E-06	1.73E-06	1.73E-06	1.73E-06	1.73E-06	1.73E-06
F43	1.73E-06	1.73E-06	1.73E-06	1.73E-06	1.73E-06	1.73E-06	1.73E-06	1.73E-06
F44	1.73E-06	0.000293	8.3E-06	1.73E-06	1.73E-06	1.73E-06	1.73E-06	1.73E-06
F46	1.73E-06	1.73E-06	1.73E-06	1.73E-06	1.73E-06	1.73E-06	1.73E-06	1.73E-06
F47	1.73E-06	1.73E-06	1.73E-06	1.73E-06	1.73E-06	1.73E-06	1.73E-06	1.73E-06
F48	1.73E-06	1.73E-06	1.73E-06	1.73E-06	1.73E-06	1.73E-06	1.73E-06	1.73E-06
F49	1.73E-06	1.73E-06	1.73E-06	1.73E-06	1.73E-06	1.73E-06	1.73E-06	1.73E-06
+/−/=	26/0/0	15/2/9	18/1/7	22/1/3	26/0/0	26/0/0	24/0/2	26/0/0

TABLE 8. Results of 26 benchmark tasks.

	F1	F2	F3	F4	F5	F6	F7	F8	F9	F10	F11	F12	F13
CLSCA	157.48	171.38	698.76	187.58	221.93	195.63	263.98	219.96	207.42	218.79	259.12	462.25	469.67
SCA	135.21	144.85	693.77	163.79	188.71	169.90	242.04	204.11	195.22	198.21	216.90	416.98	437.88
WOA	555.78	561.20	1135.36	607.37	630.31	632.58	709.62	622.90	635.81	632.90	657.39	889.13	874.01
GWO	154.33	173.71	682.52	185.25	227.53	205.38	273.24	229.01	225.98	231.41	244.44	454.79	461.75
MFO	142.38	159.84	691.29	175.77	207.61	194.33	264.13	203.22	207.54	220.73	238.79	428.47	433.65
GSA	1945.47	1981.34	2565.05	2020.23	2109.02	2065.91	2135.61	2026.36	2077.09	2068.73	2036.13	2288.25	2285.65
BA	211.15	236.89	748.17	257.92	261.94	280.16	335.56	282.66	291.86	296.59	298.38	516.08	528.08
FA	1384.21	1523.32	1951.71	1243.44	1521.01	1535.42	1719.51	1453.85	1695.15	1472.51	1523.83	1726.84	1758.33
PSO	79.17	92.60	633.11	102.13	144.58	121.17	184.00	139.92	150.15	151.07	157.34	363.92	371.72
	F14	F15	F16	F17	F18	F19	F42	F43	F44	F46	F47	F48	F49
CLSCA	833.37	210.45	175.58	267.06	315.26	357.51	547.36	506.82	513.77	1354.99	471.31	523.18	491.51
SCA	756.93	157.09	112.29	216.51	257.51	299.18	463.23	416.76	449.00	1370.02	420.77	491.78	407.74
WOA	806.92	217.62	152.54	269.54	325.15	366.35	949.08	884.28	912.31	1850.14	755.76	822.22	915.10
GWO	816.24	175.14	137.30	248.24	288.76	333.67	534.49	484.66	525.24	1409.89	473.17	541.46	492.70
MFO	776.01	160.51	123.58	221.27	259.27	311.67	482.50	415.45	441.16	1284.33	411.05	456.10	441.48
GSA	1908.45	1361.65	1266.87	1409.34	1508.37	1501.57	2388.31	2326.24	2362.59	3209.46	1838.63	1910.47	2194.04
BA	906.90	285.65	228.88	358.04	372.28	427.99	570.50	526.77	538.87	1495.64	507.52	560.25	489.91
FA	1632.66	1097.28	989.61	1137.47	1143.53	1186.11	1801.76	1738.65	1779.80	2669.16	1395.34	1456.91	1642.05
PSO	698.51	102.06	68.27	166.81	210.09	249.43	391.05	338.19	370.32	1286.01	356.04	430.33	368.85

TABLE 9. Parameter settings for the algorithms.

Method	Population size	Maximum evaluation times	Other parameters
CLSCA	30	45,0000	$a = 2$; $r_2 \in [0\ 2\pi]$; $r_3 \in [0\ 2]$; $r_4 \in [0\ 1]$; μ=4; $C_1 \in [0\ 1]$ and $C_1 \neq 0\ 1]$
SCADE	30	45,0000	$pCR = 0.8$; $beta\_min = 0.2$; $beta\_max = 0.2$
OBSCA	30	45,0000	$a = 2$; $r_2 \in [0\ 2\pi]$; $r_3 \in [0\ 2]$
FST_PSO	30	45,0000	$Vmax$=6; $Vmin$=-6; $c1$=2; $c2$=2; $w = 0.9$;
CSSA	30	45,0000	$omicron0$=0.7; $Index$=1;
CWOA	30	45,0000	b=1; t=1; $cindex$=5

the Friedman test sorts the results of the algorithms. The comparison results of the Wilcoxon test are also listed in Table 11. The ranking obtained from the Friedman test in the last row of Table 10 shows that the CLSCA is superior to its competitors. Accordingly, the comparison results reveal that the CLSCA has the best overall performance

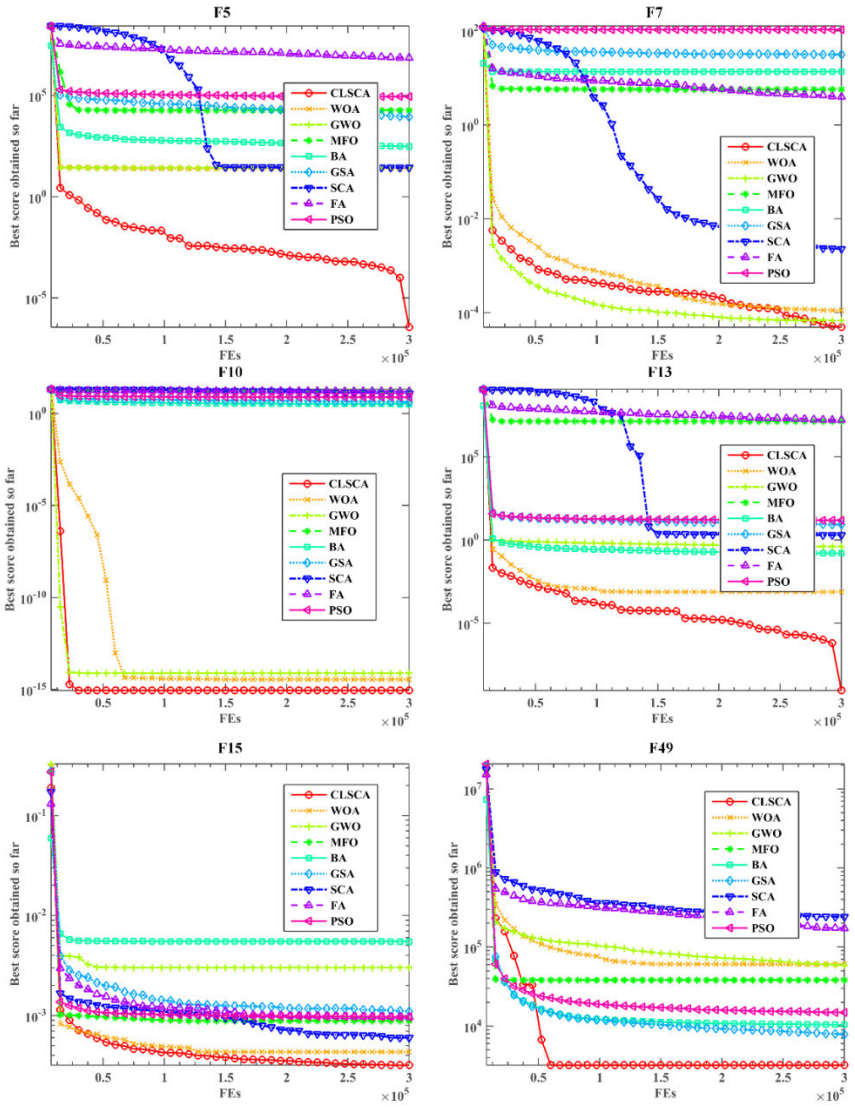

FIGURE 3. Convergence trend of the CLSCA and other algorithms.

in these tests relative to the other compared algorithms. As shown in Table 10, the CLSCA test result is 2.459302, which is the smallest compared with all the other five algorithms. The results of the Wilcoxon test in Table 11 show that the CLSCA significantly exceeds its other counterparts. According to "+/-/=" scores, it can be concluded that the CLSCA is substantially better than SCADE, OBSCA, FST_PSO, CSSA, and CWOA on 24, 28, 36, 42 and 35 out of 43 functions, respectively. Therefore, it can be concluded that the CLSCA outperforms the other compared competitors on the majority functions.

Also, the average convergence curves are compared in a logarithmic scale in Figure 4. As can be seen from the figure, the proposed CLSCA has the fastest convergence rate when dealing with all 9 testing function problems. In total, it can be concluded that CLSCA obtains the best results and convergence trends than all the other competitors over 30 independent runs.

V. CLSCA FOR THE ENGINEERING BENCHMARKS

There are several mathematical models for solving real-world problems [85-88]. In this section, the CLSCA is used to adjust engineering problems, namely, the pressure vessel design problem, the I-beam problem, and the three-bar truss problem. To fully demonstrate the efficiency of the new proposed CLSCA, the above-stated methods including the MFO, PSO, GWO, SCADE, OBSCA, CGSCA, CBA, RCBA, and PSO with an aging leader and ALCPSO from different communities are employed to make comparisons. Under the condition of constraints, models are optimized to solve the optimal value. The results of the experiments prove that the CLSCA can effectively solve the constraint problem.

TABLE 10. Comparison results of the CLSCA and five advanced algorithms.

Function	metric	CLSCA	SCADE	OBSCA	FST_PSO	CSSA	CWOA
F1	mean	0.00E+00	0.00E+00	1.13E-157	3.86E+03	3.84E-06	0.00E+00
	std.	0.00E+00	0.00E+00	6.20E-157	8.57E+02	6.76E-06	0.00E+00
F2	mean	0.00E+00	0.00E+00	1.52E-135	2.23E+01	1.35E-03	0.00E+00
	std.	0.00E+00	0.00E+00	8.33E-135	7.93E+00	9.37E-04	0.00E+00
F3	mean	0.00E+00	0.00E+00	2.53E-31	8.47E+03	3.36E-03	5.12E-01
	std.	0.00E+00	0.00E+00	1.36E-30	2.68E+03	7.54E-03	1.51E+00
F4	mean	0.00E+00	1.15E-290	4.36E-34	2.77E+01	2.64E-04	5.74E+00
	std.	0.00E+00	0.00E+00	2.17E-33	3.84E+00	3.26E-04	1.59E+01
F5	mean	3.39E-08	8.23E+00	2.75E+01	1.15E+06	1.79E-04	2.47E+01
	std.	6.47E-08	1.22E+01	3.96E-01	5.25E+05	4.65E-04	1.31E+00
F6	mean	3.93E-09	9.23E-08	3.85E+00	3.96E+03	7.78E-06	6.06E-02
	std.	5.67E-09	6.22E-08	2.96E-01	1.10E+03	1.17E-05	1.07E-01
F7	mean	3.19E-05	1.61E-04	6.48E-04	3.50E-01	1.08E-05	2.35E-04
	std.	2.73E-05	1.40E-04	4.35E-04	2.41E-01	1.24E-05	2.59E-04
F8	mean	-1.26E+04	-1.26E+04	-4.17E+03	-5.11E+03	-1.26E+04	-1.20E+04
	std.	1.54E-06	9.00E+01	2.02E+02	8.44E+02	9.06E-07	1.48E+03
F9	mean	0.00E+00	0.00E+00	0.00E+00	1.70E+02	2.54E-06	0.00E+00
	std.	0.00E+00	0.00E+00	0.00E+00	3.17E+01	3.75E-06	0.00E+00
F10	mean	8.88E-16	8.88E-16	4.44E-15	1.23E+01	3.70E-04	3.26E-15
	std.	0.00E+00	0.00E+00	0.00E+00	1.01E+00	3.65E-04	2.15E-15
F11	mean	0.00E+00	0.00E+00	0.00E+00	3.72E+01	1.41E-05	4.24E-04
	std.	0.00E+00	0.00E+00	0.00E+00	1.21E+01	1.50E-05	2.32E-03
F12	mean	1.69E-11	2.04E-09	3.75E-01	5.10E+04	2.85E-08	5.18E-03
	std.	2.51E-11	1.95E-09	1.01E-01	1.00E+05	5.44E-08	9.02E-03
F13	mean	6.10E-10	3.09E-08	2.14E+00	9.50E+05	6.50E-07	3.74E-01
	std.	1.22E-09	2.55E-08	1.44E-01	8.69E+05	1.33E-06	3.32E-01
F20	mean	3.62E+08	4.08E+08	3.77E+08	3.78E+08	1.72E+09	5.10E+07
	std.	1.11E+08	5.38E+07	9.44E+07	1.53E+08	2.30E+08	4.38E+07
F21	mean	3.17E+10	2.77E+10	2.42E+10	2.58E+10	8.68E+10	3.13E+09
	std.	5.82E+09	4.67E+09	5.05E+09	7.59E+09	9.24E+09	2.72E+09
F22	mean	4.38E+04	5.41E+04	4.75E+04	8.77E+04	8.65E+04	5.59E+04
	std.	7.49E+03	5.99E+03	6.26E+03	3.28E+04	4.00E+03	2.49E+04
F23	mean	2.34E+03	2.10E+03	2.07E+03	3.68E+03	1.90E+04	7.87E+02
	std.	7.68E+02	4.51E+02	4.70E+02	1.35E+03	3.62E+03	2.54E+02
F24	mean	5.21E+02	5.21E+02	5.21E+02	5.21E+02	5.21E+02	5.20E+02
	std.	5.15E-02	5.81E-02	3.92E-02	1.01E-01	7.85E-02	1.28E-01
F25	mean	6.32E+02	6.34E+02	6.32E+02	6.35E+02	6.44E+02	6.34E+02
	std.	2.43E+00	2.06E+00	1.20E+00	2.69E+00	1.85E+00	2.88E+00
F26	mean	9.34E+02	8.97E+02	8.88E+02	9.59E+02	1.50E+03	7.12E+02
	std.	3.68E+01	4.22E+01	3.63E+01	6.34E+01	8.91E+01	1.56E+01
F27	mean	1.06E+03	1.07E+03	1.06E+03	1.04E+03	1.16E+03	9.91E+02
	std.	1.91E+01	1.53E+01	1.32E+01	3.40E+01	2.61E+01	4.15E+01
F28	mean	1.18E+03	1.20E+03	1.19E+03	1.15E+03	1.30E+03	1.14E+03
	std.	2.08E+01	1.84E+01	1.71E+01	3.66E+01	2.51E+01	4.74E+01
F29	mean	6.89E+03	7.24E+03	6.07E+03	6.59E+03	8.70E+03	4.94E+03
	std.	4.32E+02	3.00E+02	3.75E+02	6.45E+02	4.53E+02	5.60E+02
F30	mean	8.00E+03	8.14E+03	7.24E+03	6.98E+03	9.54E+03	6.58E+03
	std.	4.21E+02	2.78E+02	4.03E+02	5.16E+02	4.92E+02	1.03E+03
F31	mean	1.20E+03	1.20E+03	1.20E+03	1.20E+03	1.20E+03	1.20E+03
	std.	3.24E-01	1.79E-01	2.97E-01	4.53E-01	6.33E-01	4.51E-01
F32	mean	1.30E+03	1.30E+03	1.30E+03	1.30E+03	1.31E+03	1.30E+03
	std.	4.09E-01	2.33E-01	3.25E-01	7.17E-01	7.95E-01	7.51E-01
F33	mean	1.48E+03	1.48E+03	1.46E+03	1.50E+03	1.68E+03	1.40E+03
	std.	1.49E+01	1.03E+01	9.49E+00	3.16E+01	2.38E+01	5.82E+00
F34	mean	1.17E+04	1.70E+04	1.32E+04	4.49E+04	2.42E+05	1.90E+03
	std.	5.45E+03	8.26E+03	8.49E+03	5.18E+04	3.98E+04	5.03E+02
F35	mean	1.61E+03	1.61E+03	1.61E+03	1.61E+03	1.61E+03	1.61E+03
	std.	2.02E-01	1.61E-01	2.27E-01	4.87E-01	2.26E-01	5.18E-01

TABLE 10. *(Continued.)* **Comparison results of the CLSCA and five advanced algorithms.**

F36	mean	8.58E+06	1.26E+07	1.02E+07	1.05E+07	2.28E+08	4.87E+06
	std.	3.83E+06	5.13E+06	5.16E+06	1.05E+07	9.66E+07	3.27E+06
F37	mean	1.23E+08	1.85E+08	1.41E+08	5.10E+07	8.84E+09	1.81E+06
	std.	5.00E+07	1.28E+08	7.04E+07	7.91E+07	3.19E+09	9.57E+06
F38	mean	2.03E+03	2.01E+03	2.01E+03	2.05E+03	2.53E+03	1.99E+03
	std.	5.91E+01	1.29E+01	1.80E+01	7.52E+01	1.39E+02	4.32E+01
F39	mean	1.48E+04	2.25E+04	2.65E+04	5.08E+04	1.93E+06	4.98E+04
	std.	5.59E+03	8.13E+03	1.05E+04	2.90E+04	2.93E+06	3.05E+04
F40	mean	1.43E+06	1.92E+06	1.54E+06	1.78E+06	1.25E+08	3.20E+06
	std.	6.89E+05	1.09E+06	6.08E+05	2.44E+06	7.98E+07	4.23E+06
F41	mean	3.04E+03	3.07E+03	3.01E+03	3.22E+03	5.88E+04	3.11E+03
	std.	1.80E+02	1.62E+02	1.61E+02	1.99E+02	7.50E+04	2.11E+02
F42	mean	2.50E+03	2.50E+03	2.68E+03	2.76E+03	2.50E+03	2.64E+03
	std.	0.00E+00	0.00E+00	1.34E+01	6.63E+01	2.78E-02	2.89E+01
F43	mean	2.60E+03	2.60E+03	2.60E+03	2.69E+03	2.60E+03	2.61E+03
	std.	0.00E+00	1.01E-06	1.52E-04	1.65E+01	2.68E-02	2.59E+01
F44	mean	2.70E+03	2.70E+03	2.70E+03	2.74E+03	2.70E+03	2.71E+03
	std.	0.00E+00	0.00E+00	1.75E-03	1.26E+01	1.16E-03	1.42E+01
F45	mean	2.72E+03	2.71E+03	2.70E+03	2.78E+03	2.79E+03	2.77E+03
	std.	3.68E+01	1.76E+01	4.63E-01	4.67E+01	2.04E+01	6.69E+01
F46	mean	2.90E+03	3.16E+03	3.23E+03	3.87E+03	4.74E+03	3.75E+03
	std.	0.00E+00	2.21E+02	3.72E+01	3.72E+02	4.33E+02	3.83E+02
F47	mean	3.00E+03	4.78E+03	5.31E+03	8.15E+03	7.18E+03	5.40E+03
	std.	0.00E+00	1.08E+03	3.68E+02	1.11E+03	3.78E+03	8.15E+02
F48	mean	3.10E+03	1.47E+07	1.43E+07	1.11E+07	5.33E+04	5.93E+06
	std.	0.00E+00	9.15E+06	7.43E+06	9.83E+06	8.65E+04	5.15E+06
F49	mean	3.20E+03	4.03E+05	3.80E+05	2.72E+05	9.71E+06	1.02E+05
	std.	0.00E+00	1.59E+05	1.23E+05	1.46E+05	7.49E+06	6.29E+04
	Ranking	2.459302	3.082558	3.425969	4.5	4.905426	2.626744

A. PRESSURE VESSEL PROBLEM

The purpose of the cylindrical pressure vessel design is to minimize the total cost and constraints by materials, structure, and welding [84]. The front end of the pressure vessel is in the shape of a hemisphere, and the ending is covered. In the pressure vessel, the optimized variables include the thickness of the shell (T_s) and the head (T_h), the inner radius (R), and the range of the section minus the head (L). The optimization model for the pressure vessel problem is expressed as follows:

$$\text{Consider } \vec{x} = [x_1 x_2 x_3 x_4] = [T_s T_h R L]$$

$$\text{Objective: } f(\vec{x})_{min} = 0.6224 x_1 x_3 x_4 + 1.7781 x_3 x_1^2 + 3.1661 x_4 x_1^2 + 19.84 x_3 x_1^2$$

$$\text{Subject to } g_1(\vec{x}) = -x_1 + 0.0193 x_3 \le 0,$$

$$g_2(\vec{x}) = -x_3 + 0.00954 x_3 \le 0,$$

$$g_3(\vec{x}) = -\pi x_4 x_3^2 - \frac{4}{3}\pi x_3^3 + 1,296,000 \le 0,$$

$$g_4(\vec{x}) = x_4 - 240 \le 0,$$

Variable ranges:

$$0 \le x_1 \le 99,$$

$$0 \le x_2 \le 99,$$

$$10 \le x_3 \le 200,$$

$$10 \le x_4 \le 200.$$

The optimization results of the CLSCA are presented in Table 12. The PSO algorithm was used to optimize the model, and the minimum cost was 6061.0777. MFO solved this mathematical model with a minimum cost of 6840.476. The GWO, SCADE, OBSCA, CGSCA, and ALCPSO were also used to solve the model. The CBA and RCBA obtained the current minimum cost of 7402.538 and 6636.429, respectively. The minimum cost of the CLSCA was 0.006625986. When T_S, T_h, R, and L were 1.455975, 0.645503, 66.06468, and 14.03413, respectively, the total cost of the cylindrical pressure vessel was 6059.887. Therefore, the CLSCA can provide optimal value for pressure vessel design models.

B. I-BEAM PROBLEM

In this section of the optimization model, the design problem of the I-beam is described. The objective is to design the minimum vertical deflection of the I-beam. The mathematical parameters of the model include the length, height, and two thicknesses. The mathematical model is described as follows:

$$\text{Consider } \vec{x} = [x_1 x_2 x_3 x_4] = [b h t_w t_f]$$

$$\text{Objective } f(\vec{x})_{\min} = \frac{5000}{\frac{t_w (h-2t_f)^3}{12} + \frac{b t_f^3}{6} + 2 b t_f \left(\frac{h-t_f}{2}\right)^2}$$

$$\text{Subject to } g(\vec{x}) = 2 b t_w + t_w (h - 2t_f) \le 0$$

$$\text{Variable range } \quad 10 \le x_1 \le 50$$

TABLE 11. Results of the statistical comparison between CLSCA and other algorithms by the Wilcoxon test.

Function	SCADE	OBSCA	FST_PSO	CSSA	CWOA
F1	**1.00E+00**	1.73E-06	1.73E-06	1.73E-06	**1.00E+00**
F2	**1.00E+00**	1.73E-06	1.73E-06	1.73E-06	**1.00E+00**
F3	**1.00E+00**	1.73E-06	1.73E-06	1.73E-06	1.73E-06
F4	3.79E-06	1.73E-06	1.73E-06	1.73E-06	1.73E-06
F5	1.73E-06	1.73E-06	1.73E-06	1.73E-06	1.73E-06
F6	1.92E-06	1.73E-06	1.73E-06	1.92E-06	1.73E-06
F7	4.73E-06	1.73E-06	1.73E-06	4.53E-04	3.32E-04
F8	1.73E-06	1.73E-06	1.73E-06	**6.89E-01**	1.73E-06
F9	**1.00E+00**	1.00E+00	1.73E-06	1.73E-06	**1.00E+00**
F10	**1.00E+00**	4.32E-08	1.73E-06	1.73E-06	4.78E-05
F11	**1.00E+00**	**1.00E+00**	1.73E-06	1.73E-06	**1.00E+00**
F12	1.73E-06	1.73E-06	1.73E-06	1.92E-06	1.73E-06
F13	1.73E-06	1.73E-06	1.73E-06	1.92E-06	1.73E-06
F20	4.49E-02	**7.34E-01**	**6.73E-01**	1.73E-06	1.73E-06
F21	1.57E-02	2.41E-04	5.67E-03	1.73E-06	1.73E-06
F22	8.47E-06	4.49E-02	7.69E-06	1.73E-06	2.07E-02
F23	**1.65E-01**	**1.36E-01**	8.19E-05	1.73E-06	1.92E-06
F24	**8.94E-01**	**5.86E-01**	1.73E-06	6.64E-04	1.73E-06
F25	7.27E-03	**1.85E-01**	1.59E-03	1.73E-06	**1.71E-01**
F26	2.58E-03	1.89E-04	**1.41E-01**	1.73E-06	1.73E-06
F27	**4.65E-01**	**8.22E-02**	2.41E-04	1.73E-06	2.88E-06
F28	5.29E-04	4.39E-03	1.83E-03	1.73E-06	2.41E-03
F29	3.38E-03	2.60E-06	**8.97E-02**	1.73E-06	1.73E-06
F30	**2.45E-01**	6.34E-06	1.02E-05	1.73E-06	8.47E-06
F31	**5.86E-01**	9.71E-05	3.41E-05	2.16E-05	1.73E-06
F32	1.83E-03	9.71E-05	7.27E-03	1.73E-06	1.73E-06
F33	**7.19E-01**	3.41E-05	2.61E-04	1.73E-06	1.73E-06
F34	1.17E-02	**8.29E-01**	4.86E-05	1.73E-06	1.73E-06
F35	2.61E-04	**7.66E-01**	**2.54E-01**	2.84E-05	4.39E-03
F36	8.73E-03	**1.25E-01**	**6.88E-01**	1.73E-06	3.59E-04
F37	3.33E-02	**3.93E-01**	3.32E-04	1.73E-06	1.73E-06
F38	**1.06E-01**	**1.16E-01**	**1.20E-01**	1.73E-06	5.71E-04
F39	1.06E-04	4.73E-06	2.13E-06	1.73E-06	2.60E-06
F40	**6.27E-02**	**4.17E-01**	**8.13E-01**	1.73E-06	**1.20E-01**
F41	**4.17E-01**	**4.41E-01**	7.16E-04	1.73E-06	**1.06E-01**
F42	**1.00E+00**	1.73E-06	1.73E-06	1.73E-06	2.56E-06
F43	**2.50E-01**	1.73E-06	1.73E-06	1.73E-06	1.73E-06
F44	**1.00E+00**	**5.00E-01**	1.73E-06	1.73E-06	9.77E-04
F45	**7.19E-02**	**5.71E-02**	6.34E-06	3.18E-06	**1.03E-01**
F46	1.96E-04	1.73E-06	1.73E-06	1.73E-06	1.73E-06
F47	2.70E-05	1.73E-06	1.73E-06	1.73E-06	1.73E-06
F48	1.73E-06	1.73E-06	1.73E-06	1.73E-06	1.73E-06
F49	1.73E-06	1.73E-06	1.73E-06	1.73E-06	1.73E-06
+/−/=	24/0/19	28/0/15	36/0/7	42/0/1	35/0/8

$$10 \leq x_2 \leq 80$$
$$0.9 \leq x_3 \leq 5$$
$$0.9 \leq x_4 \leq 5$$

The group of state-of-the-art SCA variants, including SCADE, OBSCA, and CGSCA, were used to optimize the mathematical model, and the minimum cost was 0.0066694, 0.0066608, and 0.0066301, respectively. The metaheuristic algorithms MFO, PSO, and GWO algorithms were used to optimize the model, and the minimum cost was 0.006628, 0.0066265, and 0.006626. The CBA, RCBA, and ALCPSO obtained the current minimum cost of 0.0067452, 0.0066264, and 0.006632, respectively.

TABLE 12. Comparison results of the pressure vessel design problem.

Algorithm	Optimal values				Optimum cost
	T_s	T_h	R	L	
CLSCA	**1.455975**	**0.645503**	**66.0647**	**14.03413**	**6059.887**
MFO	1.207776	0.218837	44.3948	70.03841	6840.476
PSO	0.812500	0.437500	42.0913	176.7465	6061.0777
GWO	2.176906	0.614469	63.9998	15.78465	6199.028
SCADE	1.465138	0.679596	65.0882	13.36838	6126.139
OBSCA	1.541814	0.687894	66.0062	10.44164	6167.018
CGSCA	1.382175	0.65677	62.8406	22.65807	6167.424
CBA	0.71503	0.702032	11.3887	199.0193	7402.538
RCBA	0.43188	35.5233	10.5238	200	6636.429
ALCPSO	1.203479	0.629159	59.3519	39.16217	6168.995

The optimization results of the CLSCA are presented in Table 13. These results reveal that the minimum vertical deflection obtained by the CLSCA is 0.0066259.

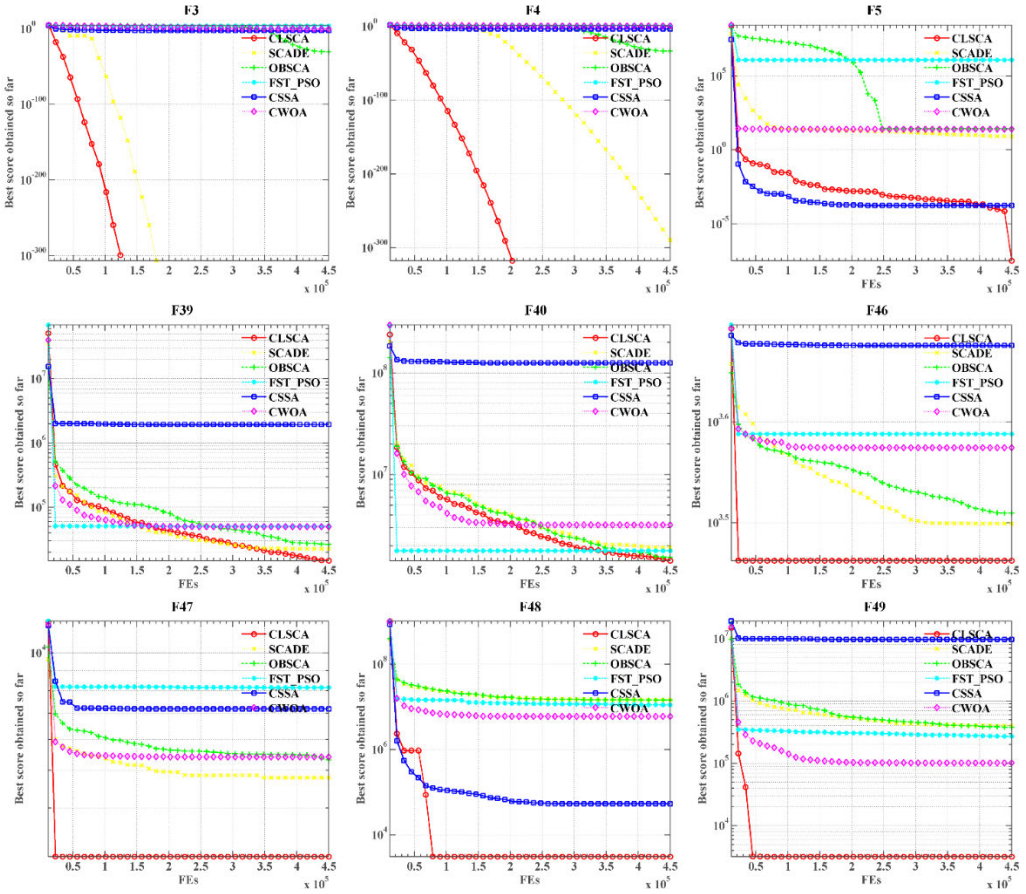

FIGURE 4. Convergence curves of the CLSCA and other advanced algorithms.

TABLE 13. Comparison results of the I-beam problem.

Algorithm	Best variables				Optimum vertical
	b	h	t_w	t_f	
CLSCA	**50**	**80**	**1.76459**	**5**	**0.0066259**
MFO	50	60.03	5	5	0.0066280
PSO	50	80	1.76254	5	0.0066265
GWO	50	80	1.76452	5	0.0066260
SCADE	50	80	1.59257	5	0.0066694
OBSCA	50	80	1.62677	5	0.0066608
CGSCA	50	80	1.74816	5	0.0066301
CBA	49.7319	79.8397	4.88498	5	0.0067452
RCBA	48.9377	79.226	2.85447	4.8721	0.0066264
ALCPSO	49.9964	79.9979	1.76335	4.9957	0.0066320

Therefore, when the four parameters are 50, 80, 1.76459, and 5, respectively, the minimum vertical deviation of the model is 0.0066259. Compared with other methods, the CLSCA optimization result is better than all the other methods, and the minimum vertical deflection value of the I-beam was obtained.

C. THREE-BAR TRUSS PROBLEM

The three-bar truss design problem is a structural optimization problem in which two parameters are used to achieve the minimum weight of stress, deflection, and buckling constraints. The mathematical model is described as follows:

TABLE 14. Comparison results of the three-bar truss problem.

Algorithm	Optimal values for variables		Optimum weight
	x_1	x_2	
CLSCA	**0.78806**	**0.40998**	**263.89636**
MFO [33]	0.78824	0.40947	263.89598
PSO	0.77268	0.46698	265.2446
GWO	0.79477	0.39192	263.987
SCADE	0.73942	0.5691	266.0501
OBSCA	0.82428	0.33314	266.4564
CGSCA	0.80812	0.36619	265.1908
CBA	0.00871	0.98083	266.5966
RCBA	0.56544	0.64079	266.6156
ALCPSO	0.999924	0.000108	282.8427

$$\text{Consider } \vec{x} = [x_1 x_2] = [A_1 A_2]$$

$$\text{Objective } f(\vec{x})_{min} = \left(2\sqrt{2}\, x_1 + x_2\right) * l$$

$$\text{Subject to } g_1(\vec{x}) = \frac{\sqrt{2}\, x_1 + x_2}{\sqrt{2}x_1^2 + 2x_1 x_2} P - \sigma \leq 0$$

$$g_2(\vec{x}) = \frac{x_2}{\sqrt{2}x_1^2 + 2x_1 x_2} P - \sigma \leq 0$$

$$g_3(\vec{x}) = \frac{1}{\sqrt{2}\, x_2 - x_1} P - \sigma \leq 0$$

Variable range $10 \leq x_1, x_2 \leq 1$, where $l = 100$ cm, $P = 2KN/\text{cm}^2$, $\sigma = 2KN/\text{cm}^2$

In this section, the CLSCA was used to solve this model and compared it with the other nine methods described above. Table 14 shows the results of CLSCA optimization when the parameters are taken as 0.78806 and 0.40998, respectively, to obtain the minimum weight of 263.89636. The results shown in Table 14 reveal that the CLSCA obtained better optimization results. Therefore, the CLSCA can handle the three-bar truss design problems very well.

VI. CONCLUSIONS AND FUTURE WORKS

The CLSCA method presented in this paper can effectively improve the performance of the original SCA method. In the proposed CLSCA, we have added a CLS strategy to enhance the ability of the algorithm to explore optimal values. Also, the Lévy flight mechanism is introduced to prevent the algorithm from prematurely falling into local optimum and improve the ability of the algorithm to search for the optimal value in the global scope. The optimization results in representative testing functions, such as unimodal functions, multimodal functions, fixed-dimension multimodal functions, hybrid functions, and composition functions, showed that the proposed CLSCA method has distinct advantages in solving the function optimization problems and can effectively improve the performance of the SCA method. Moreover, the CLSCA can achieve optimal results when solving three engineering design problems, as it was proven that the proposed algorithm could effectively deal with constraint problems.

There are still many problems that need to be further studied. First, the SCA can be combined with traditional classical meta-heuristic algorithms to improve the local and global search capabilities. Then, CLSCA can also be used to solve multi-objective problems. Also, it can be deployed on high-performance platforms with GPUs or multi-threaded processors to reduce the amount of computation of the algorithm.

VII. ACKNOWLEDGMENT

(Guoxi Liang, Huiling Chen, and Xueding Cai contributed equally to this work.)

REFERENCES

[1] Z. X. W. Liu, J. Fan, Y. Li, and L. Wang, "Evaluation of potential for salt cavern gas storage and integration of brine extraction: Cavern utilization, Yangtze river delta region," *Natural Resour. Res.*, vol. 29, Mar. 2020, doi: 10.1007/s11053-020-09640-4.

[2] J. Fan, D. Jiang, W. Liu, F. Wu, J. Chen, and J. Daemen, "Discontinuous fatigue of salt rock with low-stress intervals," *Int. J. Rock Mech. Mining Sci.*, vol. 115, pp. 77–86, Mar. 2019.

[3] Z. Zhang, D. Jiang, W. Liu, J. Chen, E. Li, J. Fan, and K. Xie, "Study on the mechanism of roof collapse and leakage of horizontal cavern in thinly bedded salt rocks," *Environ. Earth Sci.*, vol. 78, no. 10, p. 292, May 2019.

[4] W. Liu, Z. Zhang, J. Fan, D. Jiang, and J. J. K. Daemen, "Research on the stability and treatments of natural gas storage caverns with different shapes in bedded salt rocks," *IEEE Access*, vol. 8, pp. 18995–19007, 2020.

[5] J. Chen, D. Lu, W. Liu, J. Fan, D. Jiang, L. Yi, and Y. Kang, "Stability study and optimization design of small-spacing two-well (SSTW) salt caverns for natural gas storages," *J. Energy Storage*, vol. 27, Feb. 2020, Art. no. 101131.

[6] W. Liu, Z. Zhang, J. Chen, J. Fan, D. Jiang, D. Jjk, and Y. Li, "Physical simulation of construction and control of two butted-well horizontal cavern energy storage using large molded rock salt specimens," *Energy*, vol. 185, pp. 682–694, Oct. 2019.

[7] W. Liu, Z. Zhang, J. Chen, D. Jiang, F. Wu, J. Fan, and Y. Li, "Feasibility evaluation of large-scale underground hydrogen storage in bedded salt rocks of China: A case study in jiangsu province," *Energy*, vol. 198, May 2020, Art. no. 117348.

[8] W. Qiao, K. Huang, M. Azimi, and S. Han, "A novel hybrid prediction model for hourly gas consumption in supply side based on improved whale optimization algorithm and relevance vector machine," *IEEE Access*, vol. 7, pp. 88218–88230, 2019.

[9] W. Qiao, W. Tian, Y. Tian, Q. Yang, Y. Wang, and J. Zhang, "The forecasting of PM2.5 using a hybrid model based on wavelet transform and an improved deep learning algorithm," *IEEE Access*, vol. 7, pp. 142814–142825, 2019.

[10] L. Jinlong, X. Wenjie, Z. Jianjing, L. Wei, S. Xilin, and Y. Chunhe, "Modeling the mining of energy storage salt caverns using a structural dynamic mesh," *Energy*, vol. 193, Feb. 2020, Art. no. 116730.

[11] W. Qiao and Z. Yang, "An improved dolphin swarm algorithm based on kernel fuzzy C-means in the application of solving the optimal problems of large-scale function," *IEEE Access*, vol. 8, pp. 2073–2089, 2020.

[12] W. Qiao and Z. Yang, "Modified dolphin swarm algorithm based on chaotic maps for solving high-dimensional function optimization problems," *IEEE Access*, vol. 7, pp. 110472–110486, 2019.

[13] W. Qiao and Z. Yang, "Solving large-scale function optimization problem by using a new Metaheuristic algorithm based on quantum dolphin swarm algorithm," *IEEE Access*, vol. 7, pp. 138972–138989, 2019.

[14] M. Wang and H. Chen, "Chaotic multi-swarm whale optimizer boosted support vector machine for medical diagnosis," *Appl. Soft Comput.*, vol. 88, Mar. 2020, Art. no. 105946, doi: 10.1016/j.asoc.2019.105946.

[15] H. Chen, Q. Zhang, J. Luo, Y. Xu, and X. Zhang, "An enhanced bacterial foraging optimization and its application for training kernel extreme learning machine," *Appl. Soft Comput.*, vol. 86, Jan. 2020, Art. no. 105884, doi: 10.1016/j.asoc.2019.105884.

[16] Q. Li, H. Chen, H. Huang, X. Zhao, Z. Cai, C. Tong, W. Liu, and X. Tian, "An enhanced grey wolf optimization based feature selection wrapped kernel extreme learning machine for medical diagnosis," *Comput. Math. Methods Med.*, vol. 2017, pp. 1–15, Jan. 2017.

[17] X. Zhang, D. Wang, Z. Zhou, and Y. Ma, "Robust low-rank tensor recovery with rectification and alignment," *IEEE Trans. Pattern Anal. Mach. Intell.*, early access, 2019, doi: 10.1109/TPAMI.2019.2929043.

[18] S. Mirjalili and A. Lewis, "The whale optimization algorithm," *Adv. Eng. Softw.*, vol. 95, pp. 51–67, May 2016.

[19] H. Chen, Y. Xu, M. Wang, and X. Zhao, "A balanced whale optimization algorithm for constrained engineering design problems," *Appl. Math. Model.*, vol. 71, pp. 45–59, Jul. 2019.

[20] J. Luo, H. Chen, A. A. Heidari, Y. Xu, Q. Zhang, and C. Li, "Multi-strategy boosted mutative whale-inspired optimization approaches," *Appl. Math. Model.*, vol. 73, pp. 109–123, Sep. 2019.

[21] H. Chen, C. Yang, A. A. Heidari, and X. Zhao, "An efficient double adaptive random spare reinforced whale optimization algorithm," *Expert Syst. Appl.*, Oct. 2019, Art. no. 113018, doi: 10.1016/j.eswa.2019.113018.

[22] X. S. Yang, "A new metaheuristic bat-inspired algorithm," in *Studies in Computational Intelligence*, vol. 284. Berlin, Germany: Springer, 2010, pp. 65–74.

[23] H. Yu, N. Zhao, P. Wang, H. Chen, and C. Li, "Chaos-enhanced synchronized bat optimizer," *Appl. Math. Model.*, vol. 77, pp. 1201–1215, Jan. 2020.

[24] R. Storn and K. Price, "Differential evolution—A simple and efficient heuristic for global optimization over continuous spaces," *J. Global Optim.*, vol. 11, no. 4, pp. 341–359, 1997.

[25] W.-T. Pan, "A new fruit fly optimization algorithm: Taking the financial distress model as an example," *Knowl.-Based Syst.*, vol. 26, pp. 69–74, Feb. 2012.

[26] X. Zhang, Y. Xu, C. Yu, A. A. Heidari, S. Li, H. Chen, and C. Li, "Gaussian mutational chaotic fruit fly-built optimization and feature selection," *Expert Syst. Appl.*, vol. 141, Mar. 2020, Art. no. 112976.

[27] H. Chen, S. Li, A. A. Heidari, P. Wang, J. Li, Y. Yang, M. Wang, and C. Huang, "Efficient multi-population outpost fruit fly-driven optimizers: Framework and advances in support vector machines," *Expert Syst. Appl.*, vol. 142, Mar. 2020, Art. no. 112999.

[28] H. Huang, X. A. Feng, S. Zhou, J. Jiang, H. Chen, and Y. Li, "A new fruit fly optimization algorithm enhanced support vector machine for diagnosis of breast cancer based on high-level features," *BMC Bioinf.*, vol. 20, Jun. 10 2019.

[29] L. Shen, H. Chen, Z. Yu, W. Kang, B. Zhang, H. Li, B. Yang, and D. Liu, "Evolving support vector machines using fruit fly optimization for medical data classification," *Knowl.-Based Syst.*, vol. 96, pp. 61–75, Mar. 2016.

[30] S. Mirjalili, "Moth-flame optimization algorithm: A novel nature-inspired heuristic paradigm," *Knowl.-Based Syst.*, vol. 89, pp. 228–249, Nov. 2015.

[31] M. Wang, H. Chen, B. Yang, X. Zhao, L. Hu, Z. Cai, H. Huang, and C. Tong, "Toward an optimal kernel extreme learning machine using a chaotic moth-flame optimization strategy with applications in medical diagnoses," *Neurocomputing*, vol. 267, pp. 69–84, Dec. 2017.

[32] Y. Xu, H. Chen, A. A. Heidari, J. Luo, Q. Zhang, X. Zhao, and C. Li, "An efficient chaotic mutative moth-flame-inspired optimizer for global optimization tasks," *Expert Syst. Appl.*, vol. 129, pp. 135–155, Sep. 2019.

[33] Y. Xu, H. Chen, J. Luo, Q. Zhang, S. Jiao, and X. Zhang, "Enhanced moth-flame optimizer with mutation strategy for global optimization," *Inf. Sci.*, vol. 492, pp. 181–203, Aug. 2019.

[34] X. Zhao, D. Li, B. Yang, C. Ma, Y. Zhu, and H. Chen, "Feature selection based on improved ant colony optimization for online detection of foreign fiber in cotton," *Appl. Soft Comput.*, vol. 24, pp. 585–596, Nov. 2014.

[35] W. Deng, J. Xu, and H. Zhao, "An improved ant colony optimization algorithm based on hybrid strategies for scheduling problem," *IEEE Access*, vol. 7, pp. 20281–20292, 2019.

[36] Z. Cai, J. Gu, J. Luo, Q. Zhang, H. Chen, Z. Pan, Y. Li, and C. Li, "Evolving an optimal kernel extreme learning machine by using an enhanced grey wolf optimization strategy," *Expert Syst. Appl.*, vol. 138, Dec. 2019, Art. no. 112814.

[37] M. Wang, H. Chen, H. Li, Z. Cai, X. Zhao, C. Tong, J. Li, and X. Xu, "Grey wolf optimization evolving kernel extreme learning machine: Application to bankruptcy prediction," *Eng. Appl. Artif. Intell.*, vol. 63, pp. 54–68, Aug. 2017.

[38] X. Zhao, X. Zhang, Z. Cai, X. Tian, X. Wang, Y. Huang, H. Chen, and L. Hu, "Chaos enhanced grey wolf optimization wrapped ELM for diagnosis of paraquat-poisoned patients," *Comput. Biol. Chem.*, vol. 78, pp. 481–490, Feb. 2019.

[39] J. Luo, H. Chen, Q. Zhang, Y. Xu, H. Huang, and X. Zhao, "An improved grasshopper optimization algorithm with application to financial stress prediction," *Appl. Math. Model.*, vol. 64, pp. 654–668, Dec. 2018.

[40] Y. Chen, L. Li, X. Zhao, J. Xiao, Q. Wu, and Y. Tan, "Simplified hybrid fireworks algorithm," *Knowl.-Based Syst.*, vol. 173, pp. 128–139, Jun. 2019.

[41] J. Kennedy and R. Eberhart, "Particle swarm optimization," in *Proc. IEEE Int. Conf. Neural Netw. Conf. Proc.*, Nov./Dec. 1995, pp. 1942–1948.

[42] Y. Chen, L. Li, J. Xiao, Y. Yang, J. Liang, and T. Li, "Particle swarm optimizer with crossover operation," *Eng. Appl. Artif. Intell.*, vol. 70, pp. 159–169, Apr. 2018.

[43] W. Deng, H. Zhao, X. Yang, J. Xiong, M. Sun, and B. Li, "Study on an improved adaptive PSO algorithm for solving multi-objective gate assignment," *Appl. Soft Comput.*, vol. 59, pp. 288–302, Oct. 2017.

[44] S. Mirjalili, A. H. Gandomi, S. Z. Mirjalili, S. Saremi, H. Faris, and S. M. Mirjalili, "Salp swarm algorithm: A bio-inspired optimizer for engineering design problems," *Adv. Eng. Softw.*, vol. 114, pp. 163–191, Dec. 2017.

[45] A. A. Heidari, S. Mirjalili, H. Faris, I. Aljarah, M. Mafarja, and H. Chen, "Harris hawks optimization: Algorithm and applications," *Future Gener. Comput. Syst.*, vol. 97, pp. 849–872, Aug. 2019, doi: 10.1016/j.future.2019.02.028.

[46] H. Chen, S. Jiao, M. Wang, A. A. Heidari, and X. Zhao, "Parameters identification of photovoltaic cells and modules using diversification-enriched Harris hawks optimization with chaotic drifts," *J. Cleaner Prod.*, vol. 244, Jan. 2020, Art. no. 118778.

[47] H. M. Ridha, A. A. Heidari, M. Wang, and H. Chen, "Boosted mutation-based Harris hawks optimizer for parameters identification of single-diode solar cell models," *Energy Convers. Manage.*, vol. 209, Apr. 2020, Art. no. 112660.

[48] X. Xu and H.-L. Chen, "Adaptive computational chemotaxis based on field in bacterial foraging optimization," *Soft Comput.*, vol. 18, no. 4, pp. 797–807, Apr. 2014.

[49] Q. Zhang, H. Chen, A. A. Heidari, X. Zhao, Y. Xu, P. Wang, Y. Li, and C. Li, "Chaos-induced and mutation-driven schemes boosting salp chains-inspired optimizers," *IEEE Access*, vol. 7, pp. 31243–31261, 2019.

[50] Q. Zhang, H. Chen, J. Luo, Y. Xu, C. Wu, and C. Li, "Chaos enhanced bacterial foraging optimization for global optimization," *IEEE Access*, vol. 6, pp. 64905–64919, 2018.

[51] S. Mirjalili, "SCA: A sine cosine algorithm for solving optimization problems," *Knowl.-Based Syst.*, vol. 96, pp. 120–133, Mar. 2016.

[52] J. Tu, A. Lin, H. Chen, Y. Li, and C. Li, "Predict the entrepreneurial intention of fresh graduate students based on an adaptive support vector machine framework," *Math. Problems Eng.*, vol. 2019, pp. 1–16, Jan. 2019.

[53] H. Chen, M. Wang, and X. Zhao, "A multi-strategy enhanced sine cosine algorithm for global optimization and constrained practical engineering problems," *Appl. Math. Comput.*, vol. 369, Mar. 2020, Art. no. 124872, doi: 10.1016/j.amc.2019.124872.

[54] A. Lin, Q. Wu, A. A. Heidari, Y. Xu, H. Chen, W. Geng, Y. Li, and C. Li, "Predicting intentions of students for master programs using a chaos-induced sine cosine-based fuzzy K-nearest neighbor classifier," *IEEE Access*, vol. 7, pp. 67235–67248, 2019.

[55] H. Chen, S. Jiao, A. A. Heidari, M. Wang, X. Chen, and X. Zhao, "An opposition-based sine cosine approach with local search for parameter estimation of photovoltaic models," *Energy Convers. Manage.*, vol. 195, pp. 927–942, Sep. 2019.

[56] H. Chen, A. A. Heidari, X. Zhao, L. Zhang, and H. Chen, "Advanced orthogonal learning-driven multi-swarm sine cosine optimization: Framework and case studies," *Expert Syst. Appl.*, vol. 144, Apr. 2020, Art. no. 113113.

[57] M. A. Elaziz, D. Oliva, and S. Xiong, "An improved opposition-based sine cosine algorithm for global optimization," *Expert Syst. Appl.*, vol. 90, pp. 484–500, Dec. 2017.

[58] R. Sindhu, R. Ngadiran, Y. M. Yacob, N. A. H. Zahri, and M. Hariharan, "Sine–cosine algorithm for feature selection with elitism strategy and new updating mechanism," *Neural Comput. Appl.*, vol. 28, no. 10, pp. 2947–2958, Oct. 2017.

[59] M. A. Tawhid and V. Savsani, "Multi-objective sine-cosine algorithm (MO-SCA) for multi-objective engineering design problems," *Neural Comput. Appl.*, vol. 31, no. S2, pp. 915–929, Feb. 2019.

[60] N. Kumar, I. Hussain, B. Singh, and B. K. Panigrahi, "Single sensor-based MPPT of partially shaded PV system for battery charging by using cauchy and Gaussian sine cosine optimization," *IEEE Trans. Energy Convers.*, vol. 32, no. 3, pp. 983–992, Sep. 2017.

[61] M. Issa, A. E. Hassanien, D. Oliva, A. Helmi, I. Ziedan, and A. Alzohairy, "ASCA-PSO: Adaptive sine cosine optimization algorithm integrated with particle swarm for pairwise local sequence alignment," *Expert Syst. Appl.*, vol. 99, pp. 56–70, Jun. 2018.

[62] S. N. Chegini, A. Bagheri, and F. Najafi, "PSOSCALF: A new hybrid PSO based on sine cosine algorithm and levy flight for solving optimization problems," *Appl. Soft Comput.*, vol. 73, pp. 697–726, Dec. 2018.

[63] H. Nenavath and R. K. Jatoth, "Hybridizing sine cosine algorithm with differential evolution for global optimization and object tracking," *Appl. Soft Comput.*, vol. 62, pp. 1019–1043, Jan. 2018.

[64] H. Nenavath, D. R. Kumar Jatoth, and D. S. Das, "A synergy of the sine-cosine algorithm and particle swarm optimizer for improved global optimization and object tracking," *Swarm Evol. Comput.*, vol. 43, pp. 1–30, Dec. 2018.

[65] R. Li, Y. Dong, Z. Zhu, C. Li, and H. Yang, "A dynamic evaluation framework for ambient air pollution monitoring," *Appl. Math. Model.*, vol. 65, pp. 52–71, Jan. 2019.

[66] R. M. Rizk-Allah, "Hybridizing sine cosine algorithm with multi-orthogonal search strategy for engineering design problems," *J. Comput. Des. Eng.*, vol. 5, no. 2, pp. 249–273, Apr. 2018.

[67] R. M. Rizk-Allah, "An improved sine–cosine algorithm based on orthogonal parallel information for global optimization," *Soft Comput.*, vol. 23, no. 16, pp. 7135–7161, Aug. 2019.

[68] K. Z. Zamli, F. Din, B. S. Ahmed, and M. Bures, "A hybrid Q-learning sine-cosine-based strategy for addressing the combinatorial test suite minimization problem," *PLoS ONE*, vol. 13, no. 5, 2018, Art. no. e0195675.

[69] J. Zhang, Y. Zhou, and Q. Luo, "An improved sine cosine water wave optimization algorithm for global optimization," *J. Intell. Fuzzy Syst.*, vol. 34, no. 4, pp. 2129–2141, Apr. 2018.

[70] G. Liu, W. Jia, M. Wang, A. A. Heidari, H. Chen, Y. Luo, and C. Li, "Predicting cervical hyperextension injury: A covariance guided sine cosine support vector machine," *IEEE Access*, vol. 8, pp. 46895–46908, 2020.
[71] G.-G. Wang, L. Guo, A. H. Gandomi, G.-S. Hao, and H. Wang, "Chaotic krill herd algorithm," *Inf. Sci.*, vol. 274, pp. 17–34, Aug. 2014.
[72] S. Mirjalili, S. M. Mirjalili, and A. Lewis, "Grey wolf optimizer," *Adv. Eng. Softw.*, vol. 69, pp. 46–61, Mar. 2014.
[73] B. Q. J. Liang and P. Suganthan, "Problem definitions and evaluation criteria for the CEC 2014 special session and competition on single objective real-parameter numerical optimization," in *Computational Intelligence Laboratory*. 2014.
[74] J. Derrac, S. García, D. Molina, and F. Herrera, "A practical tutorial on the use of nonparametric statistical tests as a methodology for comparing evolutionary and swarm intelligence algorithms," *Swarm Evol. Comput.*, vol. 1, no. 1, pp. 3–18, Mar. 2011.
[75] E. Rashedi, H. Nezamabadi-Pour, and S. Saryazdi, "GSA: A gravitational search algorithm," *Inf. Sci.*, vol. 179, no. 13, pp. 2232–2248, Jun. 2009.
[76] S. García, A. Fernández, J. Luengo, and F. Herrera, "Advanced nonparametric tests for multiple comparisons in the design of experiments in computational intelligence and data mining: Experimental analysis of power," *Inf. Sci.*, vol. 180, no. 10, pp. 2044–2064, May 2010.
[77] M. S. Nobile, P. Cazzaniga, D. Besozzi, R. Colombo, G. Mauri, and G. Pasi, "Fuzzy self-tuning PSO: A settings-free algorithm for global optimization," *Swarm Evol. Comput.*, vol. 39, pp. 70–85, Apr. 2018.
[78] G. I. Sayed, G. Khoriba, and M. H. Haggag, "A novel chaotic salp swarm algorithm for global optimization and feature selection," *Int. J. Speech Technol.*, vol. 48, no. 10, pp. 3462–3481, Oct. 2018.
[79] D. Yousri, D. Allam, and M. B. Eteiba, "Chaotic whale optimizer variants for parameters estimation of the chaotic behavior in permanent magnet synchronous motor," *Appl. Soft Comput.*, vol. 74, pp. 479–503, Jan. 2019.
[80] W. Gao, J. L. G. Guirao, M. Abdel-Aty, and W. Xi, "An independent set degree condition for fractional critical deleted graphs," *Discrete Continuous Dyn. Syst.-Series S*, vol. 12, nos. 4–5, pp. 877–886, 2019.
[81] W. Gao, J. L. G. Guirao, B. Basavanagoud, and J. Wu, "Partial multi-dividing ontology learning algorithm," *Inf. Sci.*, vol. 467, pp. 35–58, Oct. 2018.
[82] W. Gao, W. Wang, D. Dimitrov, and Y. Wang, "Nano properties analysis via fourth multiplicative ABC indicator calculating," *Arabian J. Chem.*, vol. 11, no. 6, pp. 793–801, Sep. 2018.
[83] W. Gao, H. Wu, M. K. Siddiqui, and A. Q. Baig, "Study of biological networks using graph theory," *Saudi J. Biol. Sci.*, vol. 25, no. 6, pp. 1212–1219, Sep. 2018.
[84] B. K. Kannan and S. N. Kramer, "An augmented Lagrange multiplier based method for mixed integer discrete continuous optimization and its applications to mechanical design," *J. Mech. Des.*, vol. 116, no. 2, pp. 405–411, Jun. 1994.